

Leeghwaterstraat 44
2628 CA Delft
P.O. Box 6012
2600 JA Delft
The Netherlands

www.tno.nl

T +31 88 866 22 00
F +31 88 866 06 30

TNO report

TNO 2019 R11992

Study of the heartbeat (1 minute maximum velocity) data from the building monitoring network

Date	19 December 2019
Author(s)	D. Moretti A.J. Bronkhorst C.P.W. Geurts
Number of pages	41 (incl. appendices)
Number of appendices	1
Sponsor	NAM Assen
Project name	NAM Meetnet additionele data analyses
Project number	060.34686

All rights reserved.

No part of this publication may be reproduced and/or published by print, photoprint, microfilm or any other means without the previous written consent of TNO.

In case this report was drafted on instructions, the rights and obligations of contracting parties are subject to either the General Terms and Conditions for commissions to TNO, or the relevant agreement concluded between the contracting parties. Submitting the report for inspection to parties who have a direct interest is permitted.

© 2020 TNO

Contents

1	Introduction	3
2	The building monitoring network	4
2.1	Building sensor network	4
2.2	Example of heartbeat data	8
3	Heartbeat data analysis	10
3.1	Complementary cumulative distribution function.....	10
3.2	Pre-processing of the heartbeat data	12
3.3	Selection of heartbeats corresponding with verified earthquakes.....	17
4	Results heartbeat data 01/05/2018 – 30/04/2019	24
4.1	Results complete heartbeat datasets	24
4.2	Results datasets without likely earthquake-induced heartbeats	26
5	Heartbeat data full operational period	29
5.1	Selection criteria	29
5.2	Results complete datasets	31
5.3	Results datasets without likely earthquake-induced heartbeats	33
6	Conclusion	36
7	References	37
8	Signature	38
	Appendices	
	A Processing datasets full operational period	

1 Introduction

Since 2014, a large building vibration monitoring network is in place in the province of Groningen in the North of the Netherlands [1]. The primary objective of this network is to monitor vibrations caused by shallow earthquakes, induced by natural gas production in this region. In approximately 350 buildings vibrations are measured in three orthogonal directions at foundation level in a stiff point near the corner of the building.

The measured vibrations are, in addition to earthquakes, also caused by other internal and external sources. In order to gain a better understanding of the vibration levels due to sources other than earthquakes, a detailed analysis is performed on the heartbeat data of the sensors in the monitoring network. Specific objectives of this study are:

- To determine the level of peak vibrations at various probabilities of exceedance over the period of a year, for all building sensors in the monitoring network.
- To determine the influence of induced earthquakes on the peak vibration levels.
- To determine the influence of some building characteristics (e.g. location or building typology), on the peak vibration levels.

Two heartbeat datasets are analysed:

- The heartbeat data of 254 sensors in the network for a one-year period with relatively low seismic activity ($M < 2.0$).
- The heartbeat data of 59 sensors for the complete measurement period since instalment of those sensors (about 5 years).

This report presents the results and findings of the analysis of these datasets. Chapter 2 gives a description of the building monitoring network. The analysis performed on the heartbeat data is explained in chapter 3. The results of the heartbeat data of all network sensors for the period 01/05/2018 – 30/04/2019 are presented and discussed in chapter 4. Chapter 5 presents the results of the heartbeat data analysis of a selection of sensors for their full operational lifetime. Chapter 6 gives conclusions and recommendations.

2 The building monitoring network

The monitoring network building vibrations was designed and built by TNO [1] on behalf of the NAM, with the goal to obtain more insight into the effects of earthquakes on buildings in Groningen. Figure 1 gives a schematic of the overall features of the monitoring network.

The first paragraph of this chapter gives some background on the building sensor network. The second paragraph provides information on the webform and the database containing the reasons owners specified after a trigger event (post-trigger evaluation).

General information on the buildings (e.g. soil properties, load-bearing structure, etc.) can be found in report TNO 2015 R10501 [1]. The damage inspections after each earthquake with magnitude $M \geq 2.5$ are reported in inspection reports, such as TNO 2018 R10743-B [2].

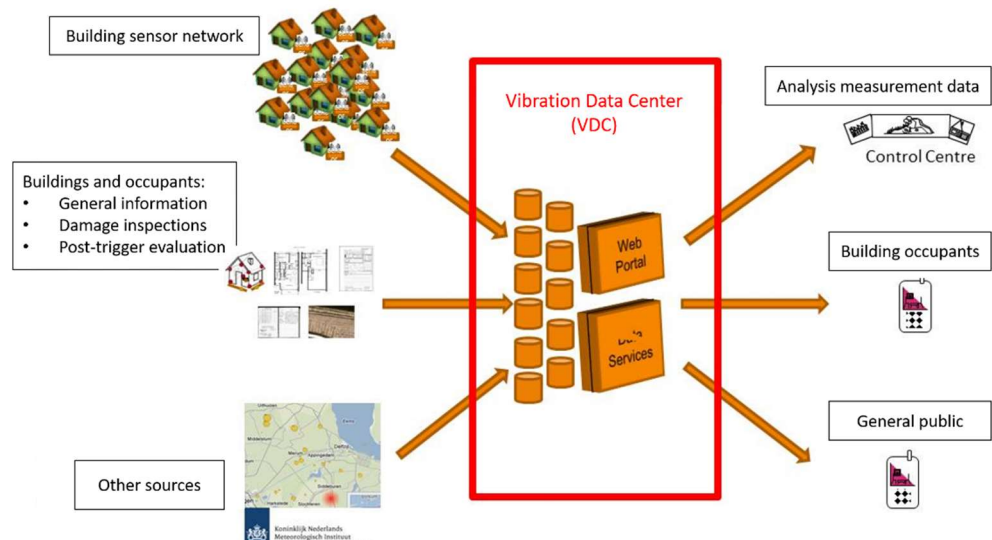


Figure 1 Schematic of the monitoring network building vibrations

2.1 Building sensor network

Figure 2(a) illustrates the approximately 350 locations in the monitoring network where vibrations are measured. The vibration measurement systems were supplied by GeoSig and consist of a recorder (GMSplus measuring system) and a tri-axial sensor (AC-73 force balance accelerometer), illustrated in Figure 3(a). The GeoSig sensors are located near a stiff corner of a building (~0.5 m) on the inside or outside, as illustrated in Figure 3(a) and (b). The X- and Y-direction of each sensor are respectively parallel and perpendicular to the façade, the Z-direction is pointing upwards. The geographic orientation of the reference system of each sensor was determined with respect to the North.

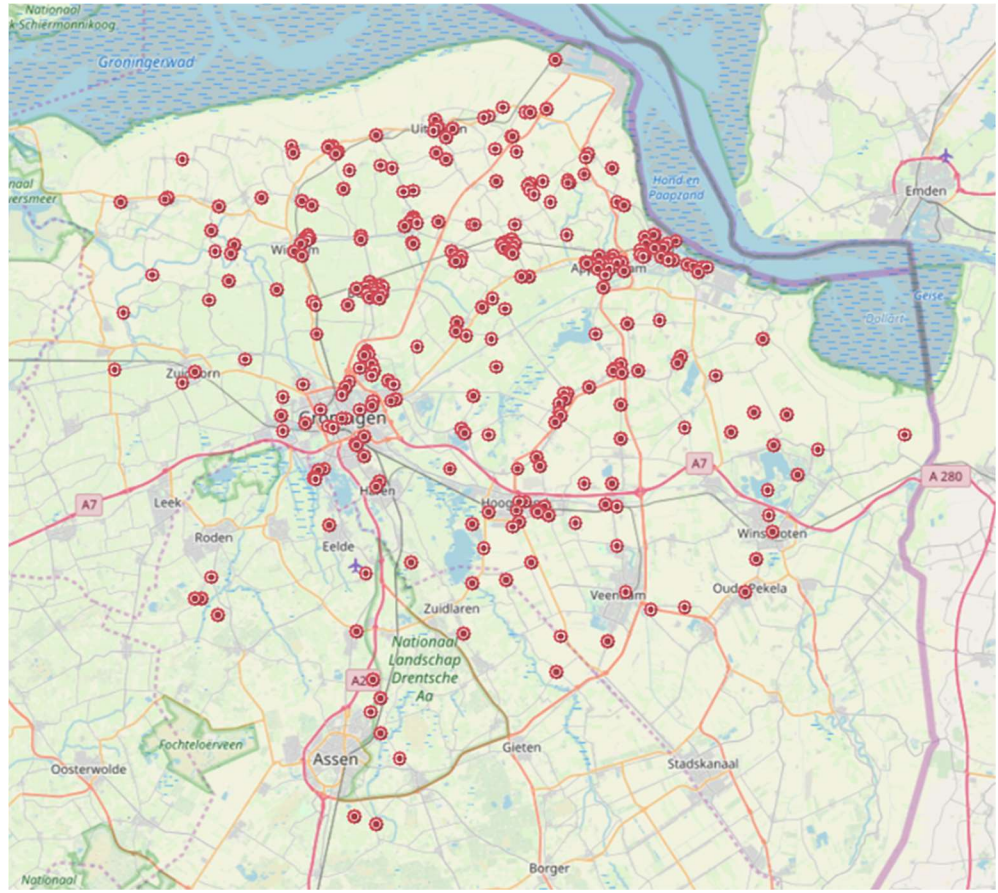


Figure 2 Vibration measurement locations in the building sensor network in Groningen.



Figure 3 (a) Geosig sensor near a stiff corner on the outside of a building, and (b) a Geosig sensor near the stiff corner inside, the large box to the left is the recorder, the small box to the right is the sensor.

The GeoSig sensors continuously sample accelerations at 250 Hz, which are automatically integrated to velocities. Each GeoSig sensor produces two output types:

- Heartbeat data
- Trigger events

In order to check that the sensor is functioning correctly it sends a “heartbeat” message every minute. This message contains information on the units health (power status, clock sync status, error messages) and the maximum accelerations and velocities in the X, Y, and Z-direction measured over the past minute. Figure 4 gives an example of a period of velocity heartbeat data.

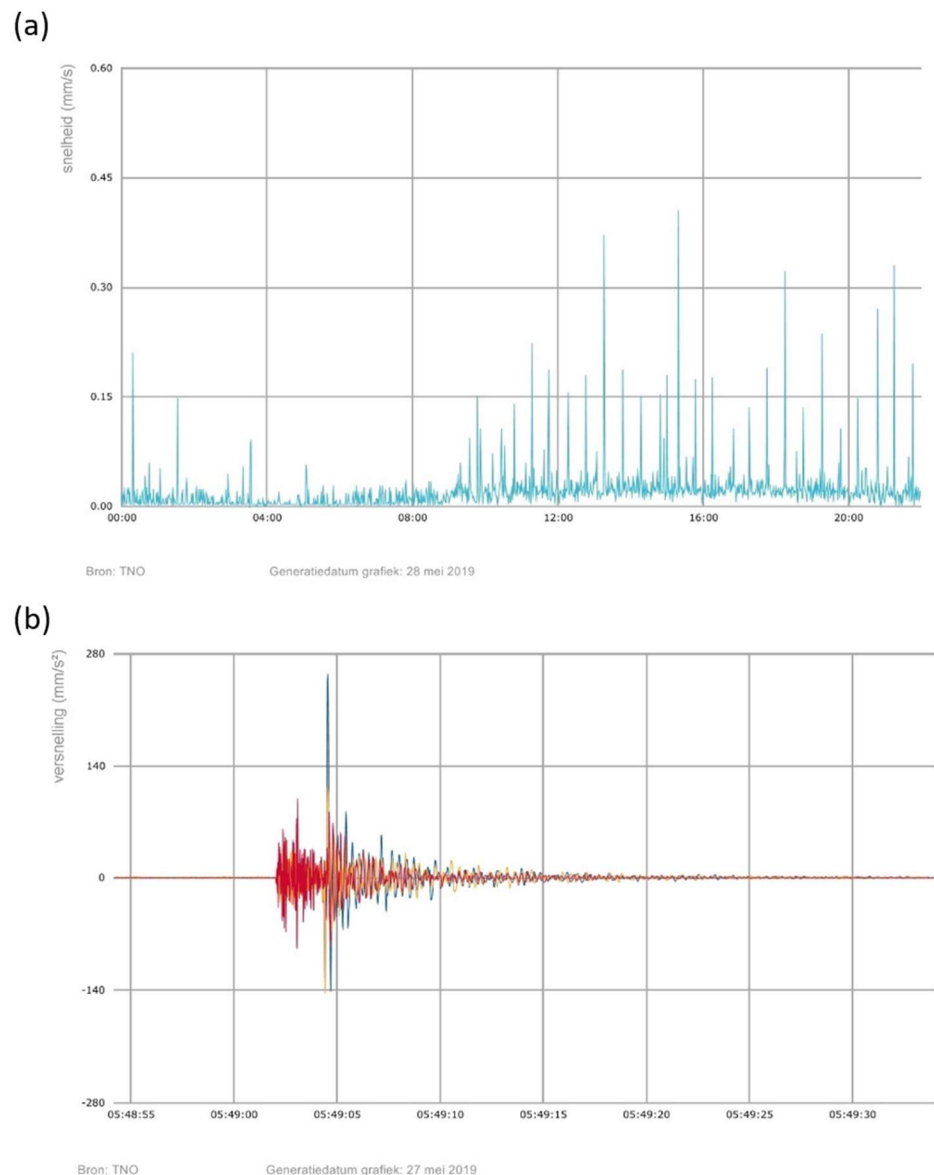


Figure 4 GeoSig sensor data send to the VDC: (a) heartbeat data and (b) trigger event.

The sensor transmits full resolution (250 Hz) data when a velocity threshold is exceeded. After the exceedance of the threshold level of 1 mm/s in X, Y, or Z-direction, the trigger time is sent to the VDC and the trigger event is logged with a pre-trigger time of 10 s. The event is recorded until 20 s after the last threshold exceedance. After the trigger event has been recorded the recorder sends the acceleration data to the Vibration Data Center (VDC), making use of the household internet connection.

The VDC was designed and build in order to receive, handle and distribute the data from the accelerometers [1]. After the data handling performed in the VDC, the results of the heartbeat data and the trigger events are presented on the website www.nam.nl. The results of the public buildings are presented at an open part of this website, and the results of the private buildings on a secured part of the website.

After each earthquake with $M \geq 2.5$, a detailed analysis is made of the trigger events caused by the earthquake [2]. This analysis is performed in combination with the damage inspections, to obtain a better understanding of the relation between the measured vibration levels and the (incremental) damage observed in some buildings. Figure 5 shows a flow chart of the analysis performed on the measured earthquake trigger events. A detailed explanation of all the computed vibration characteristics can be found in [2].

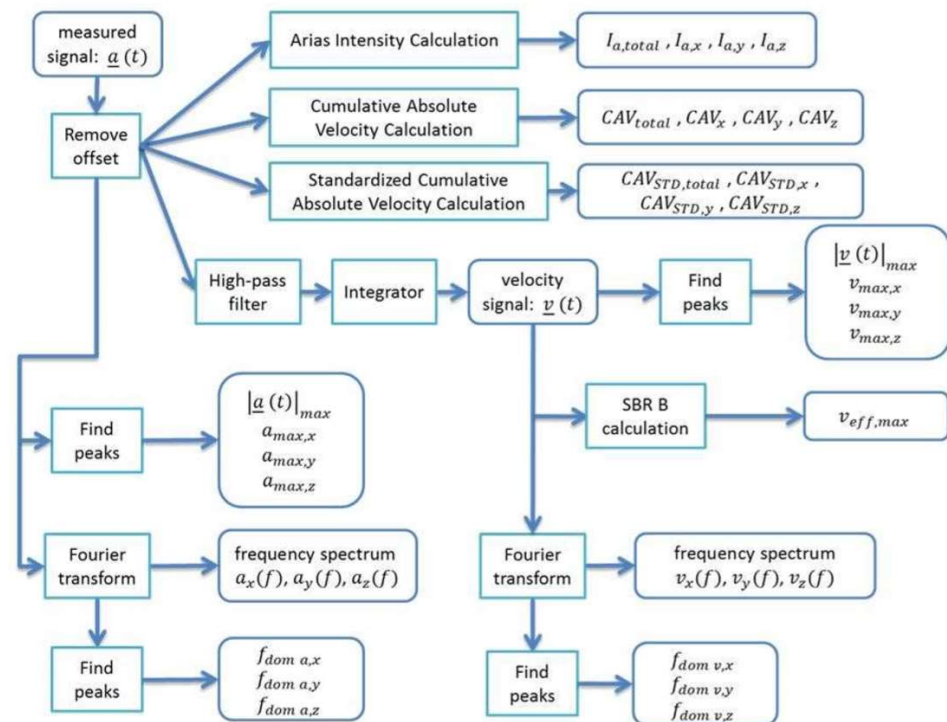


Figure 5 Flow chart of the analysis performed on the measured trigger signals of an earthquake with $M \geq 2.5$, taken from Borsje et al. [2].

2.2 Example of heartbeat data

Figure 6 shows the heartbeat data in X-direction of one of the sensors in the monitoring network for the period between 01/05/2018 and 30/04/2019. The building is about 80 m from a railroad; in front of the house there is a bus stop.

A large number of heartbeats in Figure 6 exceed the threshold of 1 mm/s, which is mainly due to the regular bus passages in front of the house. Figure 7 shows a relatively low level of vibration on nights and on Sundays (1st and 8th of July) and higher levels of vibration during the day and weekdays (e.g. 2nd to 6th of July).

Figure 8 shows another period in October and November. Between the 16th and 29th of October an increase in heartbeats above 1 mm/s is observed. In the same period the trains were temporarily replaced by a bus service [3] resulting in more vibrations.

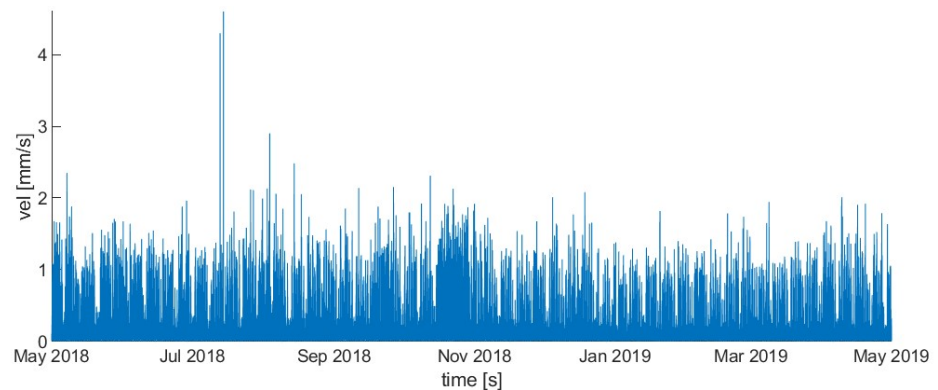


Figure 6 Heartbeat data in X-direction measured at a sensor location in the monitoring network between 01/05/2018 and 30/04/2019.

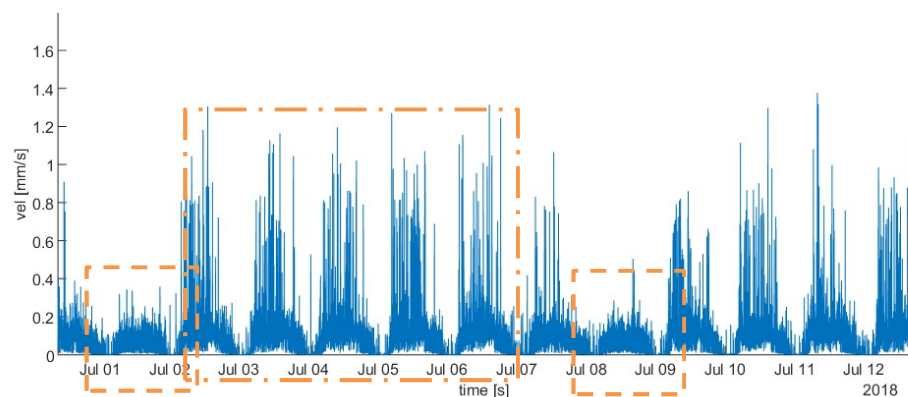


Figure 7 Detail of the vibration levels in X-direction for a period of approximately two weeks.

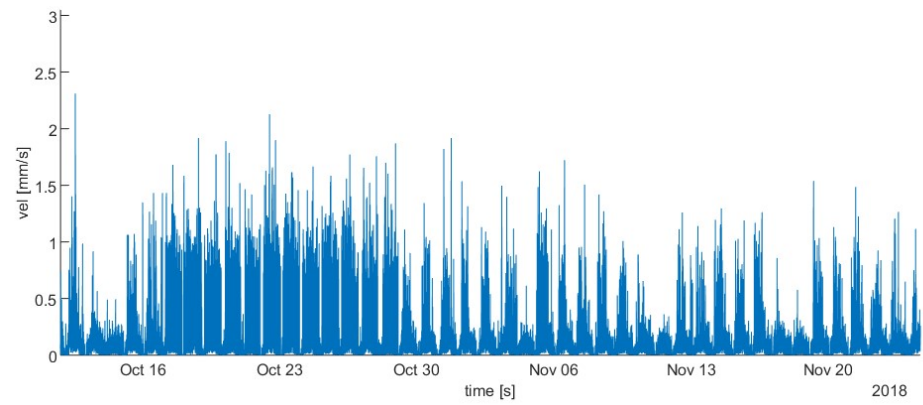


Figure 8 Detail of the vibration levels in X-direction in October and November 2018.

3 Heartbeat data analysis

This chapter explains the analysis performed on the heartbeat data. The first section describes the pre-processing performed on the heartbeat data. The second section explains the procedure to determine which heartbeats correspond with earthquakes verified by the KNMI. The last section describes the probability analysis performed on the heartbeat datasets of all buildings sensors.

3.1 Complementary cumulative distribution function

In this study, the heartbeat data is used to obtain a better understanding of how often a certain vibration level is exceeded. This is done with a complementary cumulative distribution function (CCDF). The CCDF is the complement of the cumulative distribution function (CDF). The cumulative distribution function (CDF) is used to find the probability of a variable taking a value less than or equal to x for any given function. The CCDF, being the complement to the CDF, is used to find the probability of a variable taking a value greater than x .

If $[v_x, v_y, v_z]$ represents the vector \underline{v} containing the heartbeat data, and V represents a vector with predefined velocity levels v_i , then it is possible to compute:

- The number of exceedances $N_{i,x}, N_{i,y}, N_{i,z}$ for each v_i as the number of elements in $[v_x, v_y, v_z]$ larger than v_i .
- The probability of exceedance (PE) for a reference period of 1 minute for each v_i is defined as the ratio between $N_{i,x}, N_{i,y}, N_{i,z}$ and the total number of minutes for the selected measurement period N_{tot} .

The complementary cumulative distribution functions have been computed for each direction (x, y and z) and also using an envelope of the heartbeat defined as:

$$v_{max}(t) = \max(v_x(t), v_y(t), v_z(t)) \quad \forall t \in [t_{st}, t_{end}]$$

Where t_{st} and t_{end} are the starting and ending time-stamp of the selected heartbeat data.

An example of a complementary cumulative distribution function for sensor 15 of the maximum velocity heartbeat data for the period 01-05-2018 to 30-04-2019 is shown in Figure 9. This figure shows that at the trigger level of 1 mm/s, sensor 15 recorded around 2000 exceedances.

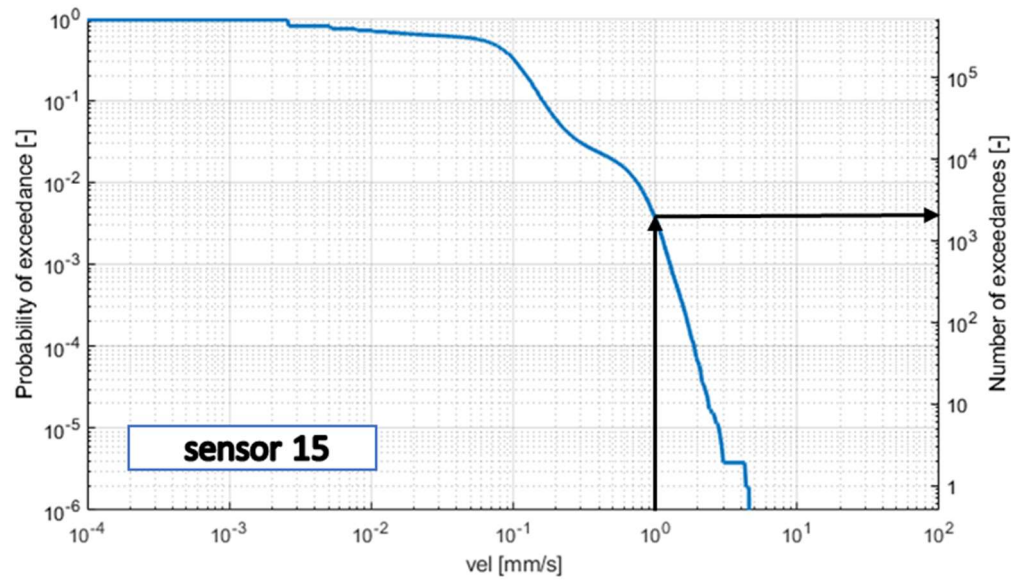


Figure 9: Example of a CCDF curve of the maximum velocity heartbeat data: on the left y-axis the probability of exceedance is plotted while on the right y-axis the number of exceedances are shown.

3.2 Pre-processing of the heartbeat data

Figure 10 shows the complementary cumulative distribution functions of the raw heartbeat data of all sensors. This figure shows two problems with the heartbeat data of some sensors:

1. Some CCDF curves reach vibration levels in the order of 1000 mm/s (bottom right of Figure 10).
2. Some CCDF curves do not reach a probability of exceedance close to 1 for low vibration velocities (top left of Figure 10).

The first problem is due to very large vibration levels in the heartbeat data, which were caused by handling of the GeoSig sensor during calibration and maintenance. The second problem is the result of missing heartbeat data over the one year period. The following paragraphs discuss these issues in more detail and explain the applied processing to obtain clean heartbeat datasets.

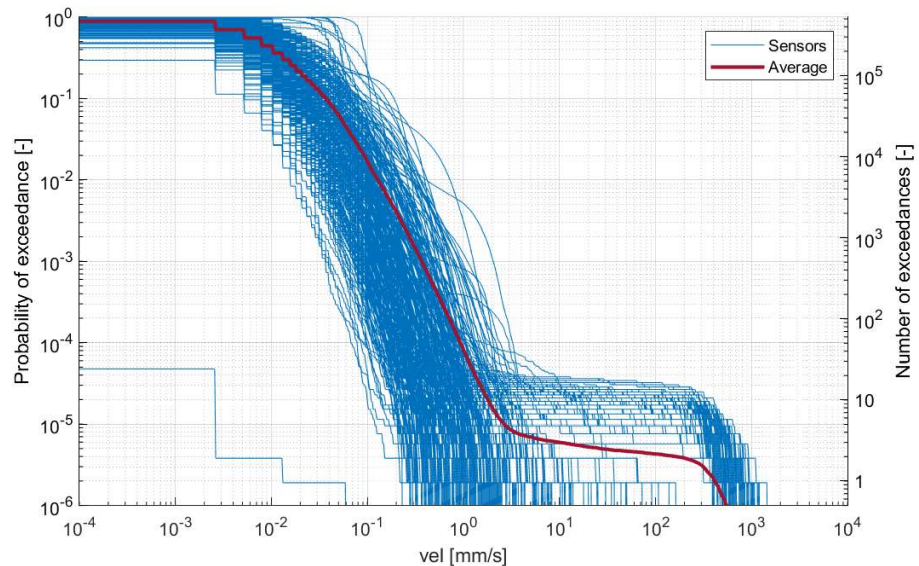


Figure 10: Envelope of the full set of one-year heartbeat data: the average CCDF (red) and the CCDF of the sensors (solid blue). In the bottom left corner a clear example of a CCDF with insufficient data, on the right a group of CCDF curves with very large vibration levels.

3.2.1 Heartbeat data spikes due to calibration and maintenance

Figure 11 (top) shows the one-year heartbeat data of one of the sensors in the network (sensor 100). On the 11th January 2019, a spike is observed in the heartbeat data. Figure 11 (middle) shows this spike consists of a period of about 15 minutes in which very large velocity levels (200 – 800 mm/s) were measured by the sensor. These vibrations are due to handling of the sensor, and not caused by vibration sources which are of interest to the current study. Therefore they need to be removed from the heartbeat datasets. Figure 3.4 (bottom) shows the one-year heartbeat dataset of sensor 100 after removal of the spikes.

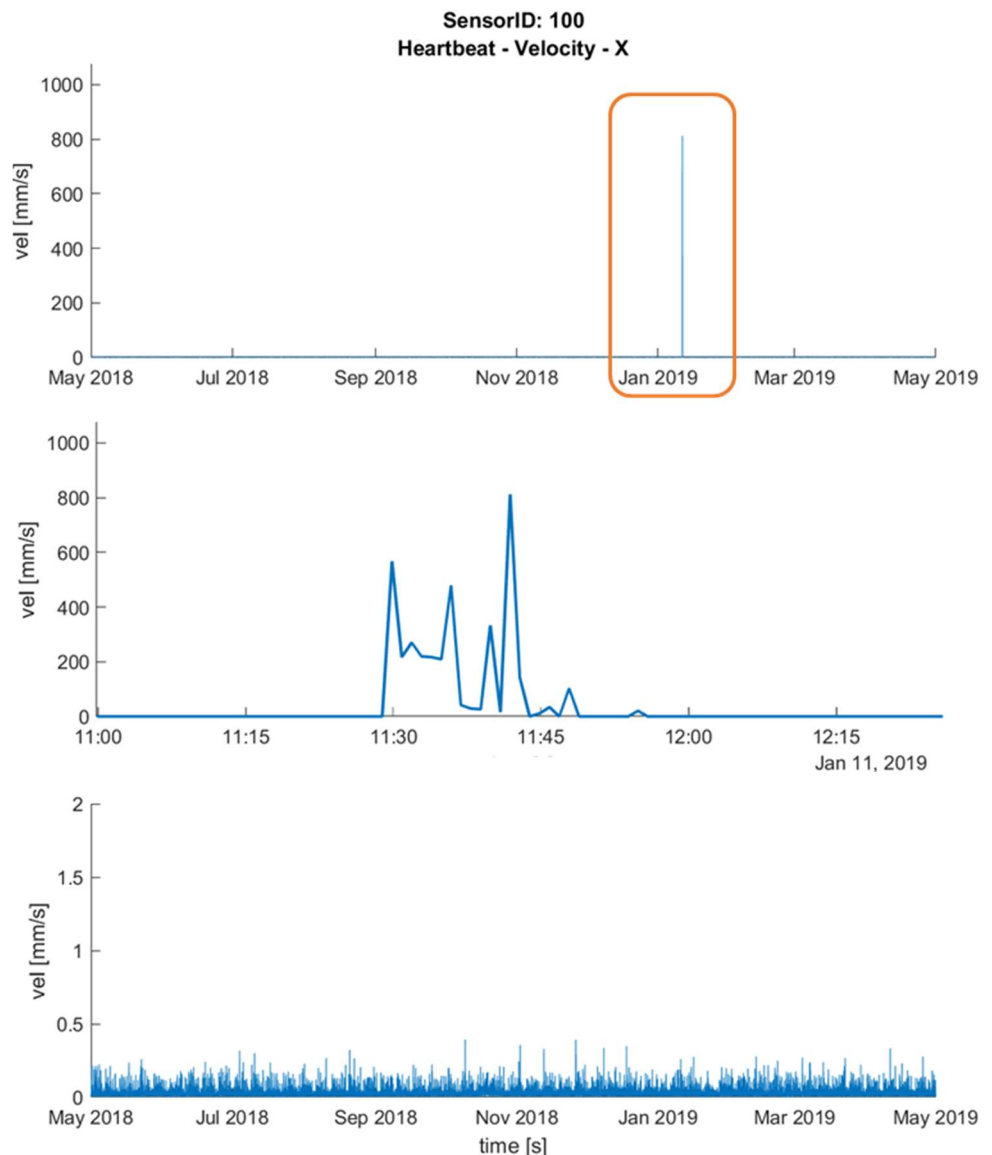


Figure 11 Velocity heartbeat data of sensor 100 in X-direction (top), a detail of the time period with the spike in the heartbeat data (middle) and the heartbeat data of sensor 100 after removal of the spike (bottom).

Figure 12 shows a bar plot of the maximum values of the heartbeat data of each sensor. A clear difference is observed for maximum velocities larger than 200 mm/s and smaller than 200 mm/s. The peaks larger than 200 mm/s could all be attributed to calibration and maintenance. The peaks smaller than 200 mm/s are due to other sources of vibrations. Of the 327 sensors 85 contain spikes due to calibration and maintenance of the sensor.

An algorithm was developed which identifies the peaks in the heartbeat data and removes a portion (-30min, +30min) of the dataset around the peaks. Figure 13 shows the effect of the removal of the spikes observed in the heartbeat data of sensor 100 on the CCDF. Figure 14 shows the CCDF curves of all heartbeat datasets after removal of the spikes.

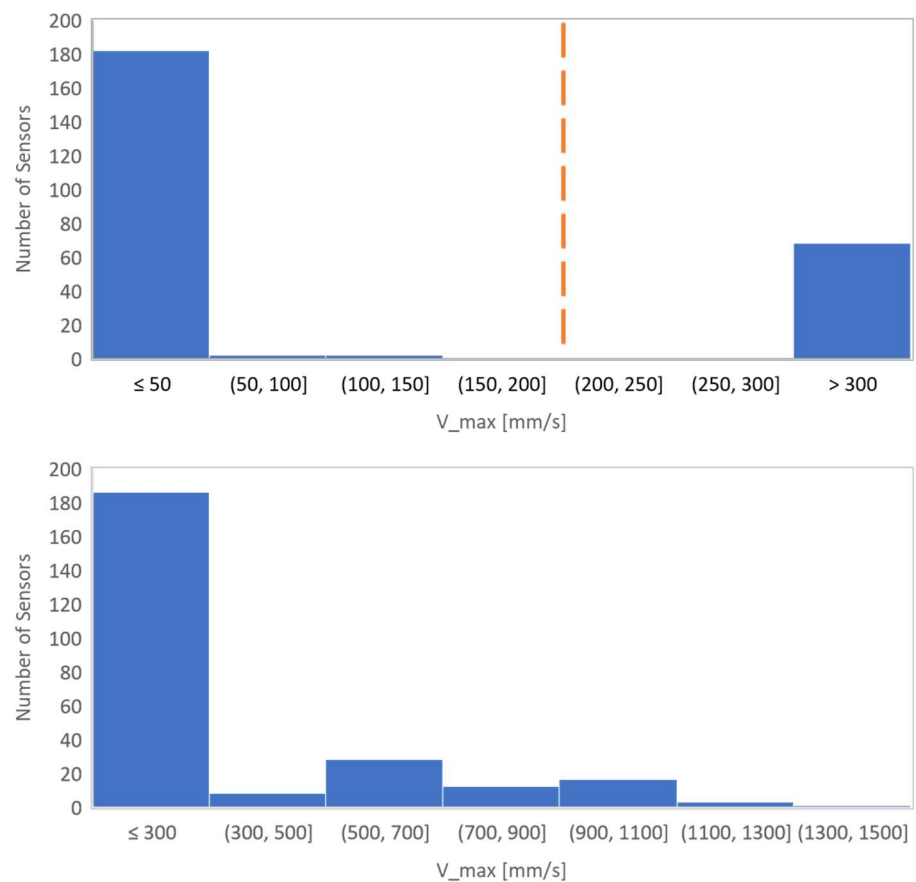


Figure 12 Maximum velocity of all the heartbeat data including the spikes. In the top figure, the 200 mm/s threshold that separates the spikes from the normal trigger events is shown while in the bottom the distribution of the maximum velocity of the spikes is presented.

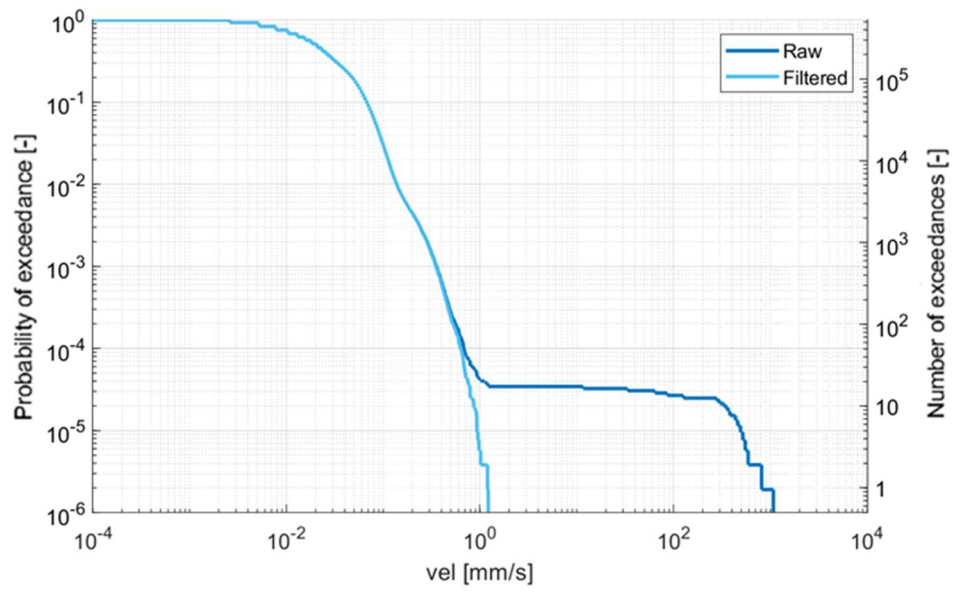


Figure 13 Comparison of the CCDF before (blue) and after (light blue) the removal of spikes.

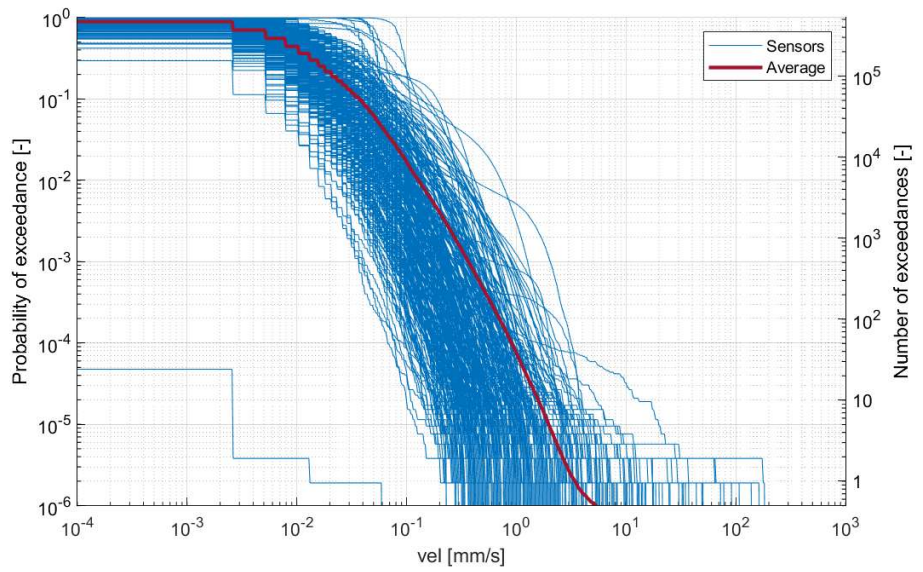


Figure 14: Envelope of the full set of one-year heartbeat data available after removal of the spikes: the average CCDF (red), the CCDF of sensor 15 (dotted blue) and of the other sensors (solid blue).

3.2.2 Sensors with missing heartbeat data

Figure 15 (top) shows the one-year heartbeat data of sensor 224. Between 25 May 2018 and 10 September 2018 no heartbeat data was recorded by this sensor. Figure 15 (bottom) shows the effect on the CCDF; the largest probability of exceedance observed on the top right is 0.68, which is significantly lower than 1.

To focus the study on the CCDF curves which are least affected by missing heartbeat data a threshold is defined. Sensors that are missing more than 2% of heartbeat data (corresponding with a period of 2 weeks) are discarded. This yielded 254 sensors with 98% or more of the one-year heartbeat data complete, and 73 heartbeat data with less than 98% (also see Figure 16).

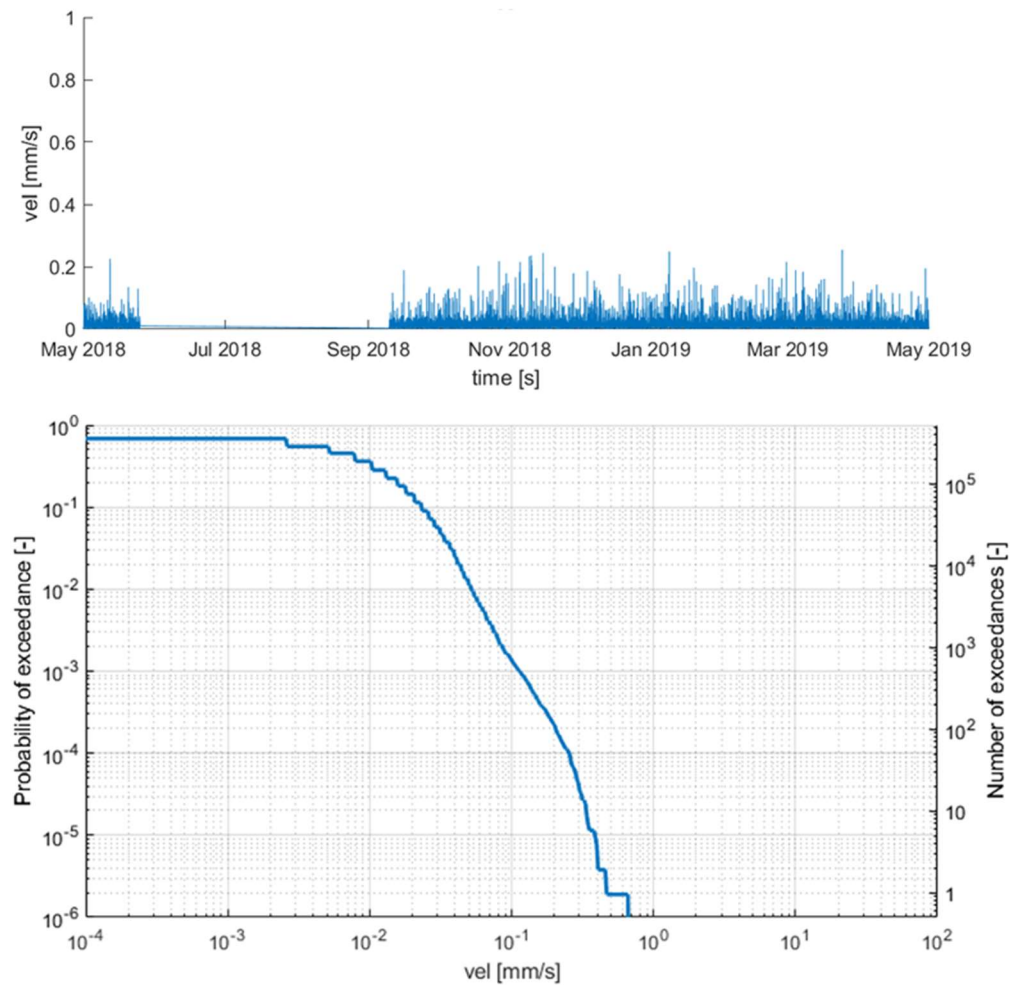


Figure 15 Velocity heartbeat data of sensor 224 in X direction: between 25 May and 10 September 2018 no heartbeat data was recorded by the sensor.

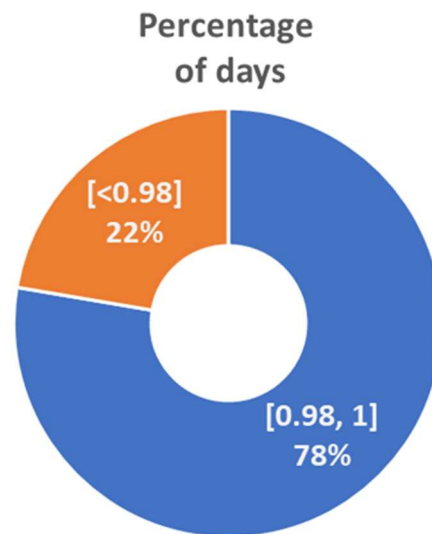


Figure 16 Pie chart of heartbeat datasets with 98% or more of the one-year heartbeat data complete (blue), and with less than 98% complete (orange).

3.3 Selection of heartbeats corresponding with verified earthquakes

To assess the influence of the earthquake events, a procedure was developed to determine the heartbeats that correspond with earthquakes verified by the KNMI. A list of earthquake events, comprising time-stamp, location (latitude and longitude), magnitude and other information is publicly available on the KNMI website (https://data.knmi.nl/datasets/aardbevingen_catalogus).

Figure 17 (top) shows a histogram of all earthquakes that were recorded in Groningen during the 1 year period between 1 May 2018 and 30 April 2019. None of these earthquakes reached a magnitude larger than $M = 2$, which means it was a year with relatively low seismicity. Figure 17 (bottom) shows the histogram of all earthquakes for the full operational period of the monitoring network.

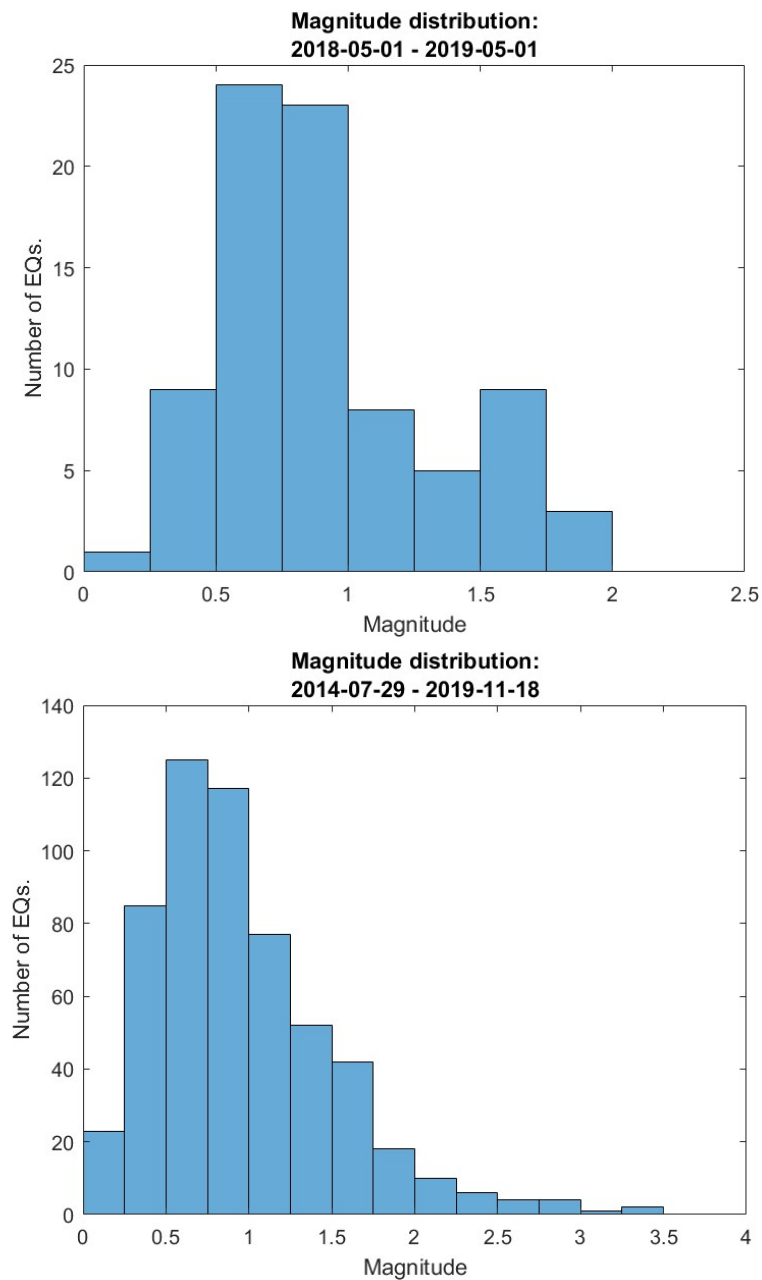


Figure 17 Histograms of the magnitude of the earthquakes recorded in Groningen (a) between 01-05-2018 and 01-05-2019, and (b) between 29-07-2014 and 18-11-2019.

In order to check if the j^{th} earthquake event of magnitude M_j could have been responsible for the recorded vibration level at sensor i around the time-stamp t_j , the “maximum expected velocity” is estimated using the empirical model described in Bommer et al. [4].

This model provides, with a certain confidence level, the maximum expected velocity in horizontal direction (i.e. the peak ground velocity, PGV) induced by an event of magnitude M_j at a certain distance D from the epicentre:

$$PGV = PGV(M_j, D)$$

The procedure compares the *PGV* estimated at a sensor location with 95% confidence intervals with the maximum velocity recorded by the sensor in the interval $\bar{t} = [t_j - 1m, t_j + 5m]$:

$$V_{max} = \max(v_x(t), v_y(t), v_z(t)) \quad \text{with } t \in \bar{t}$$

If the recorded velocity is higher than the estimated upper 95% confidence bound of the *PGV*, the vibration is unlikely to have been induced by an earthquake and . When the recorded velocity is below the upper 95% confidence bound, it is assumed to have been the result of the earthquake.

An earthquake event can coincide with periods in which no heartbeat data is available, either due to sensor maintenance (see par. 3.2.1) or because of a gap in the data (see par. 3.2.2). When the difference between the time stamp of the earthquake and the nearest heartbeat is larger than 2 minutes, no heartbeat is selected for that earthquake.

With this procedure two datasets are obtained for each sensor:

- A dataset with all heartbeat data, including those that are likely to have been caused by an earthquake.
- A dataset without heartbeat data that are likely to be the result of an earthquake.

The procedure consists of 3 steps:

1. Computation of the distance between the sensor and the event;
2. Estimation of the *PGV* with 95% confidence intervals, using the empirical equation of Bommer et al. [4];
3. Comparison of the *PGV* estimated with 95% confidence and the maximum velocity recorded in the period of the earthquake event.

The following paragraphs explain these steps in more detail.

3.3.1 *Relative distance sensor-epicentre*

Given the coordinates of the epicentre of the j^{th} earthquake event (expressed by latitude ϕ_j and longitude λ_j) and the i^{th} sensor location (given by latitude ϕ_i and longitude λ_i) the inter-distance, D_{ij} , is computed with:

$$D_{ij} = R_e \cdot c_{ij}$$

Where R_e is the radius of the earth (~6371km) and c_{ij} is determined with:

$$c_{ij} = 2 \cdot \text{atan2}(\sqrt{a}, \sqrt{1-a})$$

$$a = \sin^2\left(\frac{\phi_i - \phi_j}{2}\right) + \cos\phi_i \cdot \cos\phi_j \cdot \sin^2\left(\frac{\lambda_i - \lambda_j}{2}\right)$$

The formula to compute a is also known as the haversine formula.

3.3.2 *PGV estimate*

Let D_{ij} and M_j be respectively the inter-distance sensor-epicentre (in km) and the magnitude of the event, the empirical equation provides, with a certain level of confidence, the peak ground velocity PGV_j (in cm/s). The median is expressed by the following equations:

$$\ln(PGV_j) = c_1 + c_2 \cdot M_j + g(R_j)$$

Where R_j defines the magnitude-dependent near-source saturation of the attenuation curve and $g(R_j)$ is the geometrical spreading term:

$$R_j = \sqrt{D_{ij}^2 + [\exp(0.4233 \cdot M_j - 0.6083)]^2}$$

$$c_4 \ln(R_j) \quad R_j \leq 6.32 \text{ km}$$

$$g(R_j) = c_4 \ln(6.32) + c_{4a} \ln\left(\frac{R_j}{6.32}\right) \quad 6.32 \leq R_j \leq 11.62 \text{ km}$$

$$c_4 \ln(6.32) + c_{4a} \ln\left(\frac{11.62}{6.32}\right) + c_{4b} \ln\left(\frac{R_j}{11.62}\right) \quad R_j > 11.62 \text{ km}$$

The coefficient c_4, c_{4a}, c_{4b} have been calibrated based on three definitions of the PGV:

- the maximum of geometric means (gm) of the horizontal velocity components of all time instances;
- the maximum of the larger of the two horizontal velocity components of all time instances;
- the maximum of the velocity obtained by rotating the recorded horizontal components of all time instances.

The model is based on a lognormal distribution with a standard deviation, σ that is obtained by the combination of a between-earthquake component, τ , and a within-earthquake component, ϕ :

$$\sigma = \sqrt{\tau^2 + \phi^2}$$

The components have also been calibrated by Bommer et al. [4] for the three definitions of the peak ground velocity. The values of the calibrated coefficients can be found in Bommer et al [4].

An example of the relation between PGV and distance for the median value of the distribution is shown in Figure 18 for an earthquake of 2.5M.

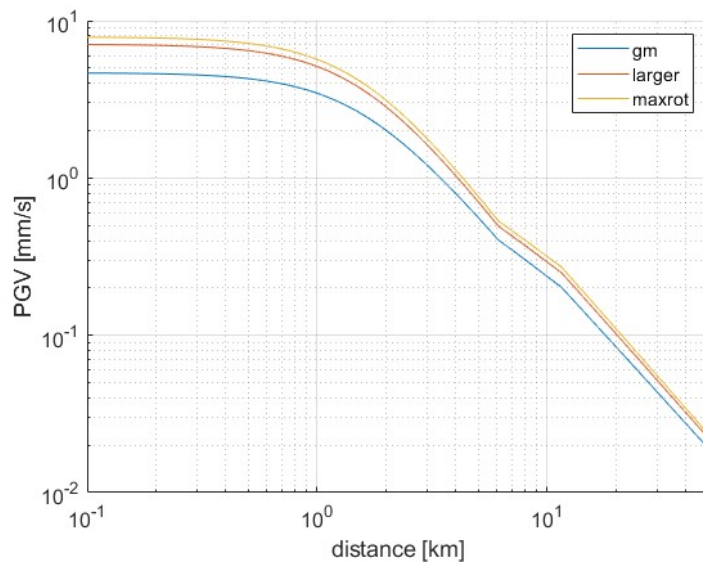


Figure 18 Median values of PGV predicted by the model described by Bommer et al. [4] against distance: geometric mean (blue), the larger component (red) and the maximum value obtained by rotating the axis (yellow).

Since the heartbeat data only provides the maximum value in X, Y and Z-direction during the minute, only the largest velocity among the three components can be computed. For this reason, the PGV is predicted with the “larger component” definition. Figure 19 shows the median, and the 66% and 95% confidence intervals obtained with the larger component definition for an earthquake with a magnitude of 2.5M.

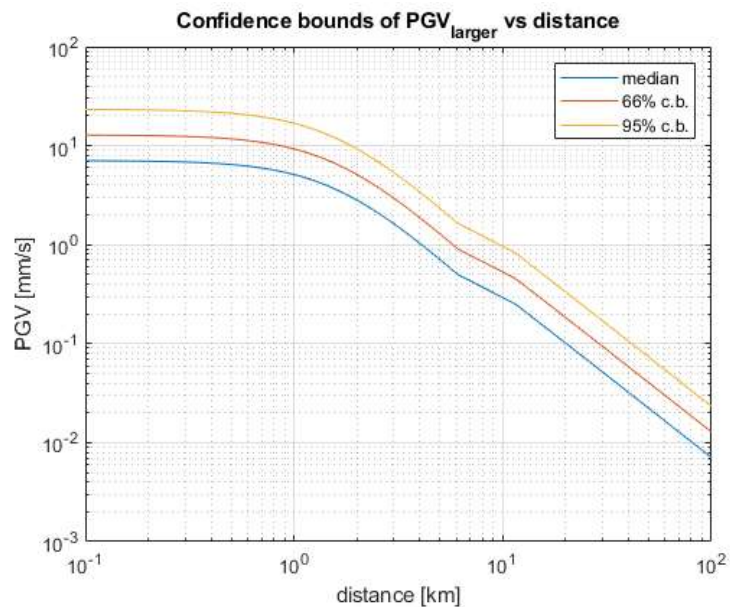


Figure 19 Confidence intervals for the PGV predicted by the “larger component” fitted model [4] against distance: median (blue), median + 1 standard deviation (red) and median + 2 standard deviation (yellow).

3.3.3 Comparison of heartbeats with the PGV estimate

To check the procedure, a comparison is made of the heartbeat data recorded in the period of the earthquake event of Garrelsweer on the 9th of June 2019 (magnitude $M = 2.5$).

Figure 20 shows the empirical PGV [4] with 95% confidence bounds at increasing distance from the epicentre of the earthquake. The data obtained during the event for 257 sensors are also plotted with red (maximum velocity in Z-direction), blue (max. velocity in Y-direction) and yellow (max. velocity in X-direction). Most of the data fall within the 95% confidence intervals, and are therefore likely to have been the result of the Garrelsweer earthquake. The good comparison in Figure 20 indicates this procedure is appropriate to determine heartbeat data that are likely to be the result of an earthquake.

Moreover, even though the empirical equation of Bommer et al. [4] was developed for horizontal velocities, Figure 20 shows none of the data in Z direction falls outside the 95% confidence bounds. This indicates that this empirical equation is also applicable for the vertical direction.

3.3.4 Examples of the heartbeat selection procedure

To illustrate the procedure used to determine whether a heartbeat might have been the result of an earthquake, this paragraph presents two examples. Figure 3.14 (top) shows a heartbeat dataset of sensor 104. Two earthquake events (A and B) are highlighted in Figure 3.14 (top). Figure 3.14 (middle) and (bottom) show detailed pictures of these events.

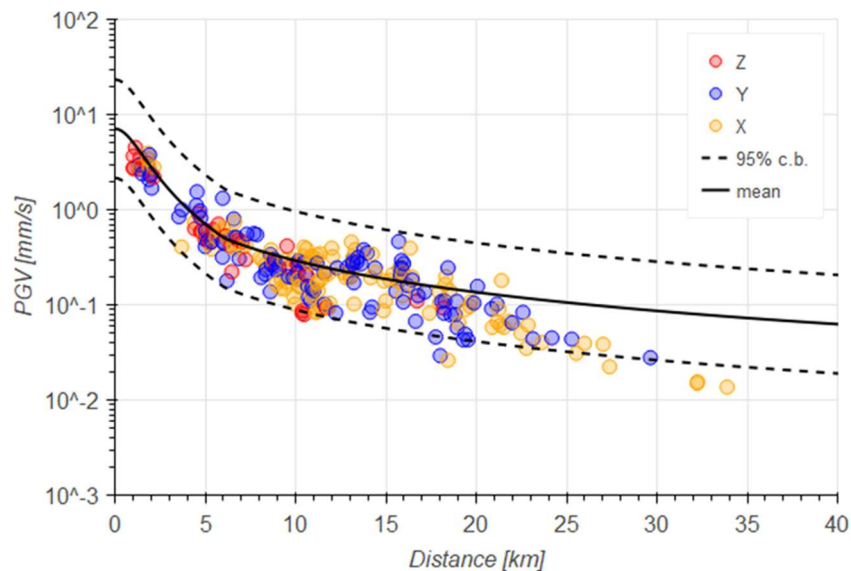


Figure 20 Comparison of the maximum velocity recorded by the sensors with the 95% confidence intervals (dotted lines) predicted with Bommer et al. [4] using the “larger component” definition for the PGV.

Detail A, illustrated in Figure 3.14 (middle), presents a situation where the PGV predicts a higher value than the one recorded by the sensor. In this case it is assumed that the heartbeat data might have been caused by the earthquake.

Detail B, illustrated in Figure 3.14 (bottom), presents a situation where the sensor recorded a velocity higher than the one estimated by the empirical PGV.: Here it is assumed that the vibration is unlikely to have been the result of the earthquake.

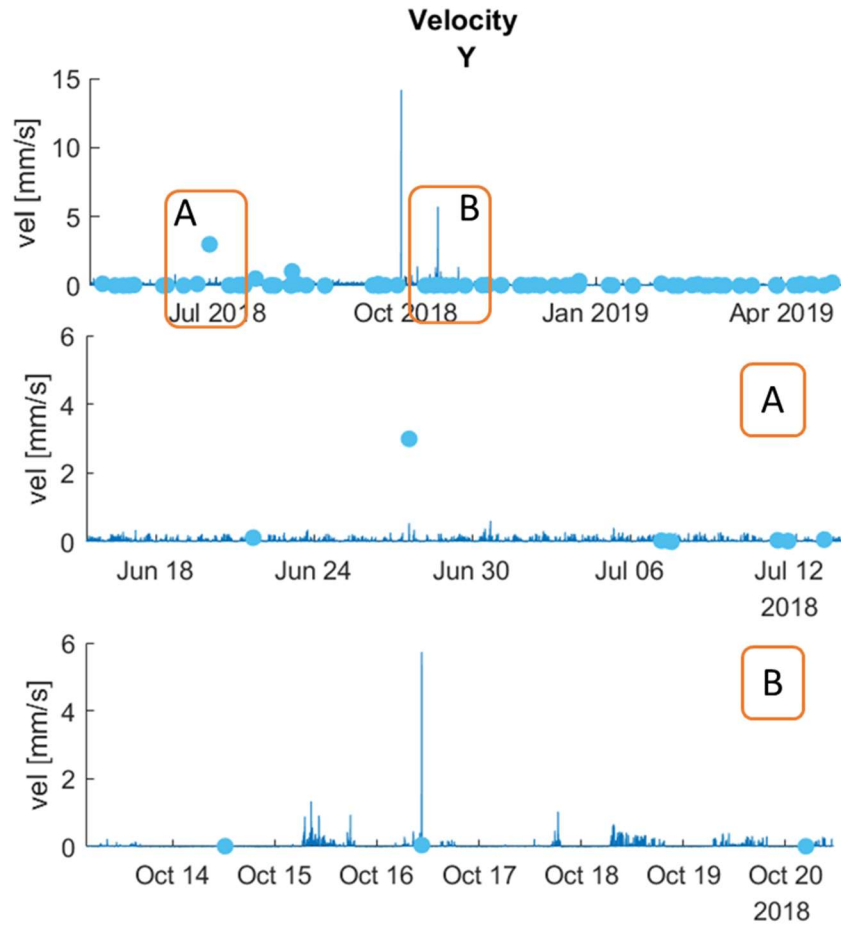


Figure 21 Heartbeat data for sensor 104 (blue line) and predicted *PGV* from the earthquake events recorded by the KNMI database (light blue dots).

4 Results heartbeat data 01/05/2018 – 30/04/2019

This chapter presents the results of the heartbeat data for all buildings in the measurement network obtained in the one-year period 01/05/2018 – 30/04/2019. During this period no earthquakes with a magnitude larger than 1.9 M were recorded. A maximum velocity was recorded close to Ten Post, on the 25th of April, 2019 at 19:27:06. In the report this dataset is referred to as the 1-year (heartbeat) dataset.

The raw heartbeat data consisted of 327 datasets collected from the same number of sensors (see Figure 2). After the processing described in chapter 3 a total of 254 heartbeat datasets remained.

The first section presents and discusses the results of the complete heartbeat datasets, including the heartbeats that are likely to be the result of an earthquake. The second section gives the results of the heartbeat datasets without the heartbeats which are likely due to an earthquake, and makes a comparison with the results obtained for the complete heartbeat datasets.

4.1 Results complete heartbeat datasets

Figure 22 shows the complementary cumulative distribution functions (CCDF) of the 254 heartbeat datasets, including heartbeats which are likely the result of an earthquake. The left vertical axis specifies the probability of exceedance, and the right vertical axis gives the number of exceedances. Highlighted in red is the average CCDF (solid red), and the lower and upper envelope (dotted red line).

Table 1 gives the number of exceedances at five velocity levels for the average CCDF and the upper and lower envelope. The velocity level of 1 mm/s corresponds with the trigger level of the building monitoring network. The levels of 3 and 5 mm/s are the lowest limits specified in SBR A [5] for a category 2 building and a category 2 building with monumental status in case of a short duration (transient) vibration signal.

On average the trigger level of the building monitoring network (1 mm/s) was exceeded 36 times per sensor in the period under investigation (1 May 2018 – 30 April 2019). The envelopes show that some of the 254 sensors did not measure any triggers events, while other sensors measured much more than the average (up to 1928 triggers). Table 1 shows that the velocity levels of 3 and 5 mm/s were on average exceeded approximately 1 time and less than 1 time in the one-year period. The 3 mm/s level was not exceeded more than 50 times at one of the 254 sensors in the one-year period; the 5 mm/s level never more than 15 times.

Table 2 gives the total number of exceedances for several velocity level ranges that were measured by the selection of 254 sensors. The trigger level (1 mm/s) was exceeded a total of 9368 times over the one-year period. The largest portion of these events did not result in an exceedance of the 3 mm/s and 5 mm/s velocity levels. The 5 mm/s velocity level was exceeded 119 times, which is 1.3% of the trigger events. Figure 22 shows that some of these events reached velocity levels much higher than 5 mm/s (up to almost 200 mm/s).

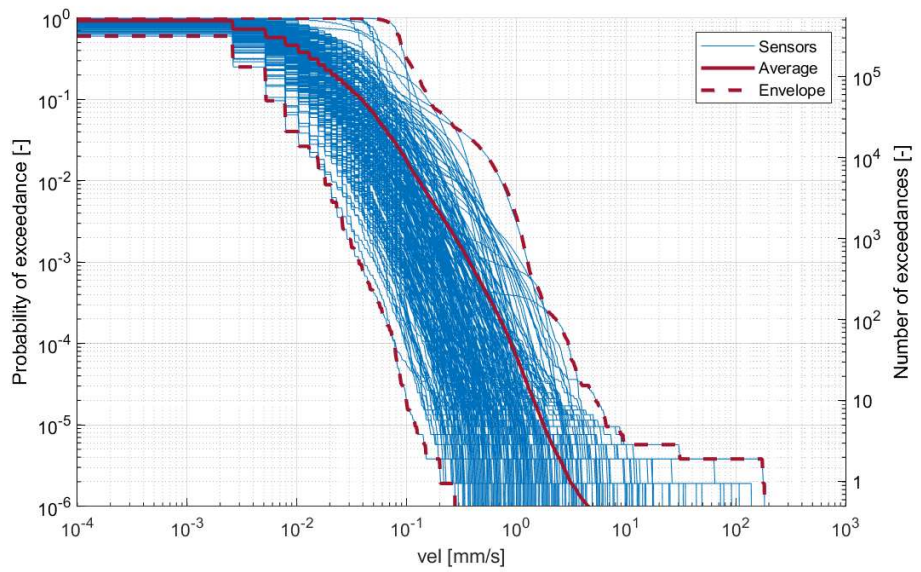


Figure 22: The CCDF curves of the 254 one-year heartbeat datasets after removing spikes and insufficient datasets.

Table 1 Number of exceedances at different velocity levels for the lower and upper envelope and the average CCDF for the one-year dataset.

Velocity level	Number of exceedances		
	Minimum	Average	Maximum
0.01 mm/s	21237	243516.9	523592
0.1 mm/s	10	9276.1	169061
1 mm/s	0	36.9	1928
3 mm/s	0	1.17	48
5 mm/s	0	0.47	13

Table 2 Total number of exceedances determined for the one-year datasets for different velocity ranges.

Velocity level range	Total number of exceedances
$1 \leq v_{max} < 3mm/s$	9071
$3 \leq v_{max} < 5mm/s$	178
$v_{max} \geq 5mm/s$	119
$v_{max} \geq 1mm/s$	9368

4.2 Results datasets without likely earthquake-induced heartbeats

The complementary cumulative distribution functions (CCDF) were also determined for the heartbeat datasets after removing a subset of heartbeats. These heartbeats were measured at the same moment as verified earthquakes by the KNMI and, based on the measured velocity level, are considered likely to be the result of an earthquake.

Figure 23 shows the CCDF of the complete dataset and of the dataset without likely earthquake-induced heartbeat. It is difficult to discern any differences between the two graphs, they look very similar. This suggests that for this one-year period, the contribution of earthquakes to the measured one-minute maximum velocity levels at the 254 sensors is low.

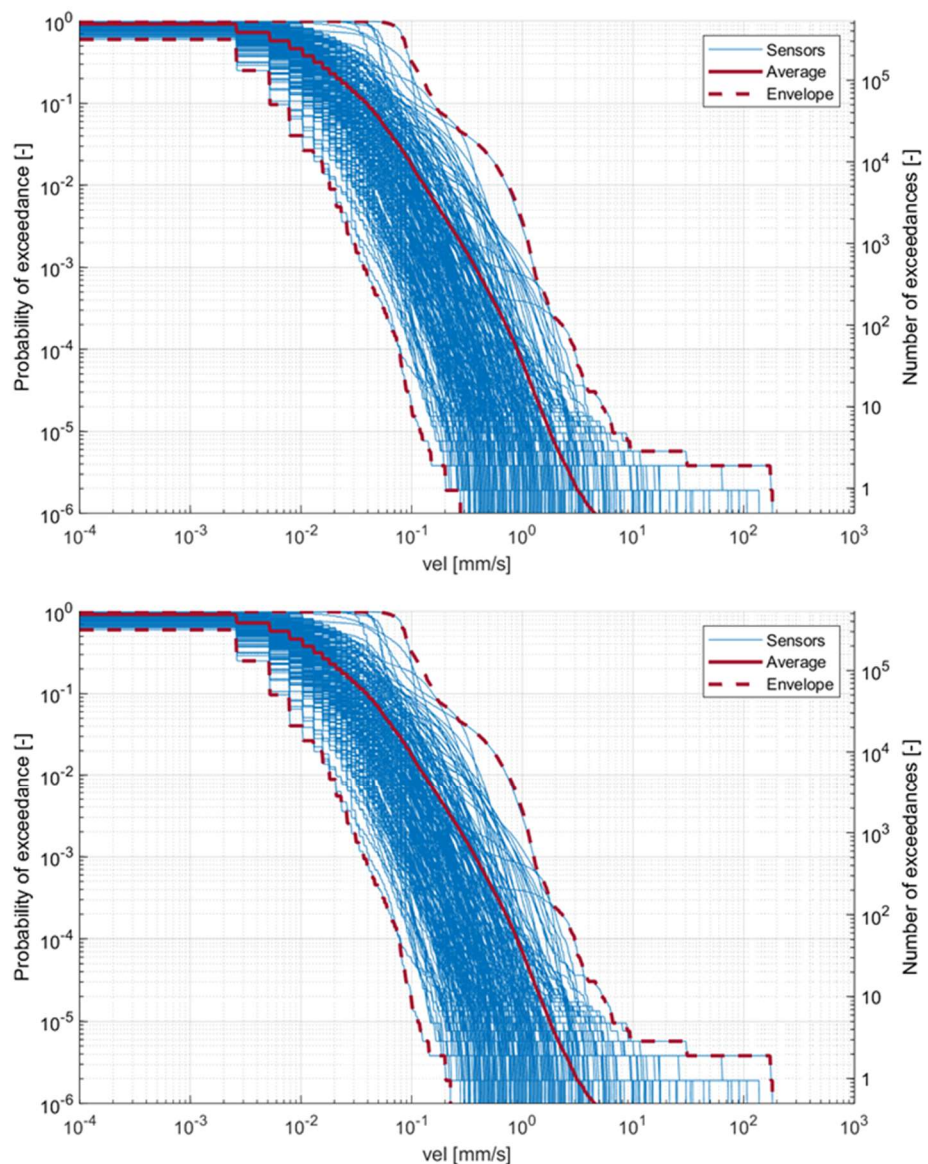


Figure 23 The CCDF curves for the complete datasets (top) and for the datasets without the likely earthquake induced heartbeats (bottom).

Figure 24 (top) presents the average CCDF and the envelope of the two heartbeat datasets. In this graph a difference is observed in the lower envelope, which is shown in more detail in Figure 24 (bottom). For sensors with relatively low vibration levels (< 1 mm/s) over the one-year period, the removal of likely earthquake-induced heartbeats has an observable effect on the number of exceedances (or probability of exceedance).

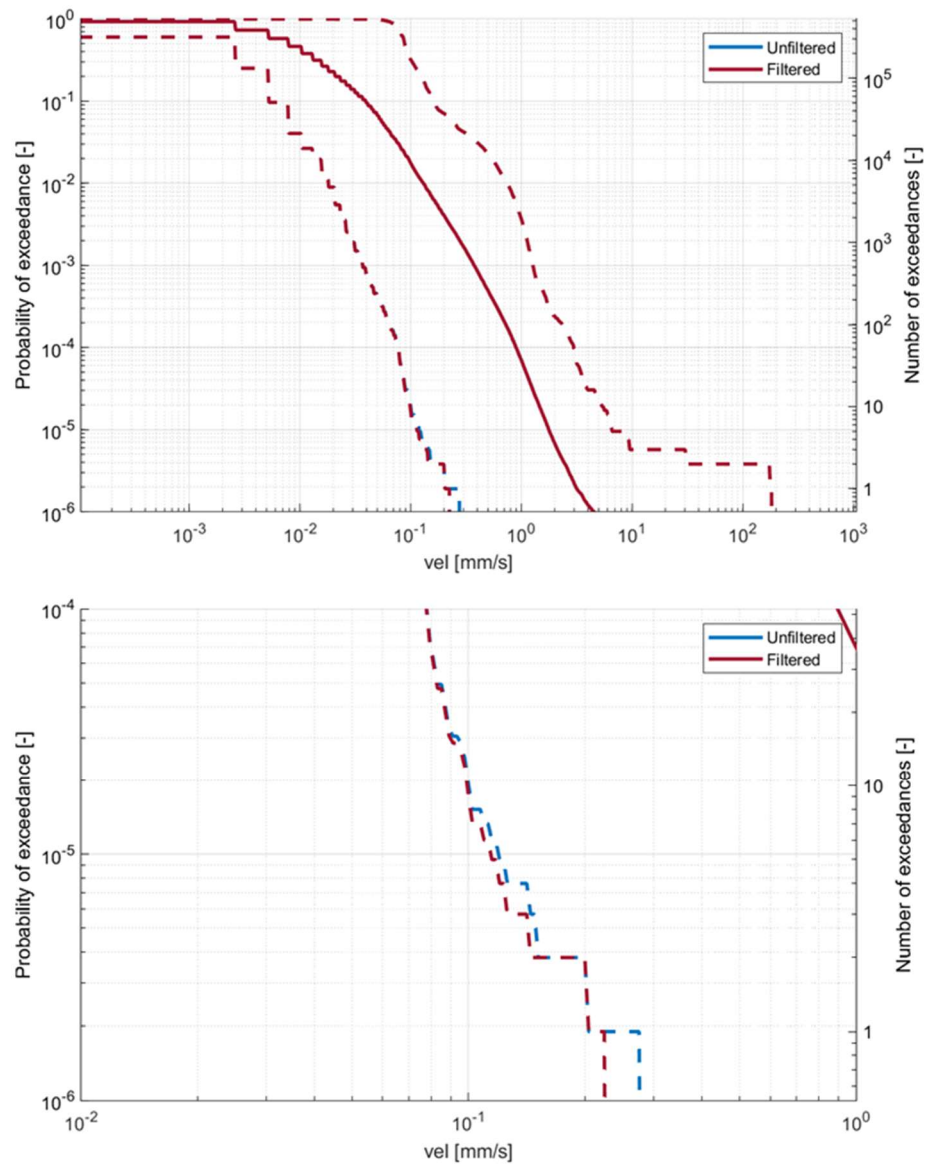


Figure 24 Comparison of average CCDF and lower and upper envelopes for the complete datasets (unfiltered) and for the datasets without (filtered) the likely earthquake induced heartbeats (top). Detail showing the difference between the filtered and unfiltered dataset in the lower envelope (bottom).

Table 3 gives the number of exceedances at various velocity levels for the average CCDF, and the lower and upper envelope of the two one-year datasets. Small differences are observed for velocity levels of 0.01 mm/s and 0.1 mm/s. For velocity levels of 1 mm/s (the trigger level), 3 mm/s and 5 mm/s no (significant) differences are observed in the number of exceedances for the average CCDF and the lower and upper envelope.

Table 4 gives the total number of exceedances measured by the 254 sensors over the one-year period for various velocity level ranges. Results are provided for the complete one-year dataset (unfiltered) and the dataset without likely earthquake-induced heartbeats (filtered). The last column gives the difference between these two datasets. For velocity levels above the trigger threshold of the monitoring network (1 mm/s), the difference between the two datasets is 16 heartbeats. This means that 0.17% of the triggers over the one-year period are likely earthquake-induced heartbeats. Table 4 furthermore shows that none of these heartbeats exceeded 3 mm/s.

Table 3 Comparison of the number of exceedances at 5 velocity levels for the lower and upper bound of the envelope and the average CCDF for the complete 1-year dataset (unfiltered) and the dataset without likely earthquake-induced heartbeats (filtered).

Velocity level	Number of exceedances					
	Minimum		Average		Maximum	
	unfiltered	filtered	unfiltered	filtered	unfiltered	filtered
0.01 mm/s	21237	21237	243516.9	243443.85	523592	523536
0.1 mm/s	10	9	9276.1	9274.16	169061	169041
1 mm/s	0	0	36.88	36.82	1928	1928
3 mm/s	0	0	1.17	1.16	48	50
5 mm/s	0	0	0.47	0.47	13	13

Table 4 Comparison of the total number of exceedances for the complete 1-year dataset (unfiltered) and the dataset without likely earthquake-induced heartbeats (filtered).for different velocity ranges.

Velocity level	Total number of exceedances (unfiltered)	Total number of exceedances (filtered)	Difference
$0.1 \leq v_{max} < 1mm/s$	2346759	2346285	474
$1 \leq v_{max} < 3mm/s$	9071	9055	16
$3 \leq v_{max} < 5mm/s$	178	178	0
$v_{max} \geq 5mm/s$	119	119	0
$v_{max} \geq 1mm/s$	9368	9352	16

5 Heartbeat data full operational period

Based on the analysis and results of the one-year dataset, a subset of sensors was selected for which the full operation period (approximately 5 years) was analysed. This chapter first explains the selection criteria, then discusses the results of the complete heartbeat datasets, and ends with a comparison of the heartbeat datasets with and without likely earthquake-induced heartbeats. Details about the (pre-)processing on the heartbeat dataset is provided in Appendix A.

5.1 Selection criteria

The selection of the sensors for which the full operational period was analysed was based on the following criteria:

- The sensor is installed before 1 January 2015.
- The one-year dataset of a sensor should miss less than 2% of data.
- The dataset for the full operational period of a sensor should contain 90% of that period.
- The selection of sensor should provide an appropriate coverage of the vibration levels observed in the one-year dataset, i.e. the selected sensor should have CCDF curves near the upper and lower envelope and near the average CCDF of the one-year dataset.
- The selection of sensors should provide a good coverage of the Groningen area.

These selection criteria yielded a total of 59 sensors. Figure 25 (top) shows the coverage of these sensors over the Groningen area. A large concentration of sensors is found near Loppersum (the centre circle). Figure 25 (bottom) shows the complementary cumulative distribution functions (CCDF) of the one-year dataset, with the CCDF curves of the 59 sensors highlighted in red. The 59 datasets are evenly spread out over the range of CCDF curves.

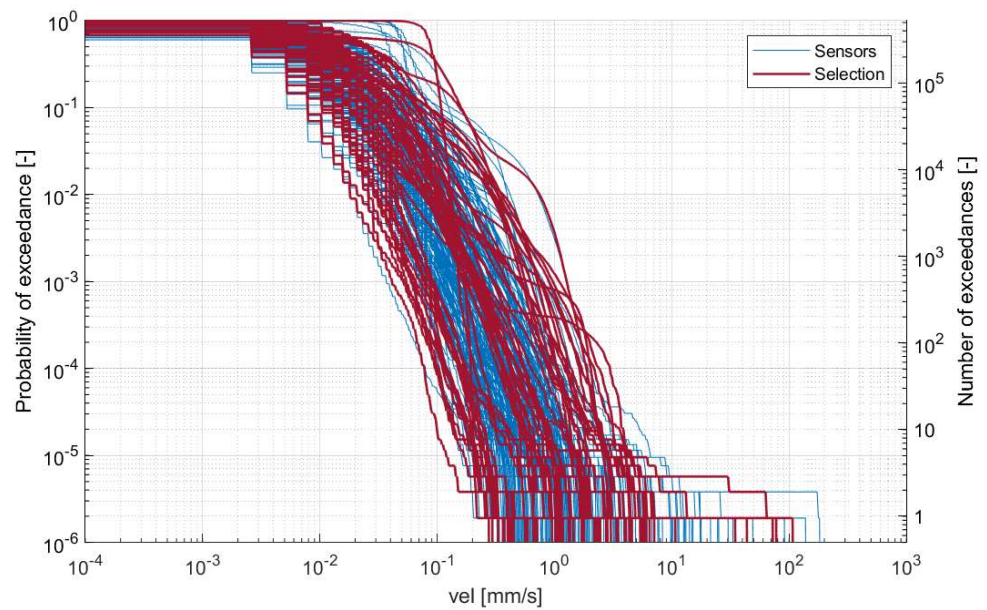
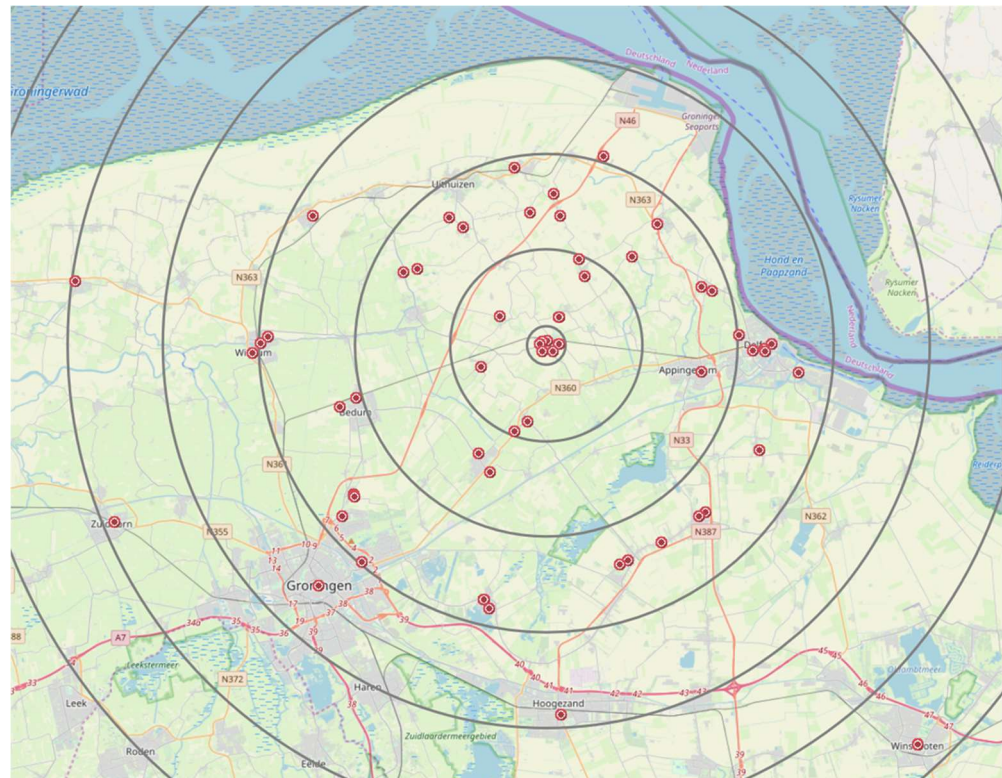


Figure 25 Position of the selected sensors for analysis of the full operational-period (top). The red dots indicate the selected sensors while the grey circles indicates the distance from Loppersum (1, 5, 10, 15, 20, 25, 30 and 40 km). All CCDF curves of the one-year dataset and of the selected sensors for the analysis of the data from the full operational period (bottom).

5.2 Results complete datasets

Figure 26 shows the complementary cumulative distribution functions (CCDF) of the 59 complete heartbeat datasets. Highlighted in red is the average CCDF (solid red), and the lower and upper envelope (dotted red line). Table 5 gives the number of exceedances at five velocity levels for the average CCDF and the upper and lower envelope.

On average the trigger level (1 mm/s) was exceeded 565 times per sensor (i.e. ~113 trigger events per sensor per year). The results for the lower envelope show that some of the 59 sensors did not measure any triggers events over their full operational period, while the upper envelope shows that other sensors measured more than 10000 triggers events (up to 12319). Table 5 shows that the velocity levels of 3 and 5 mm/s were on average exceeded approximately 6 times and 2 times per sensor per year. The largest number of exceedances of the 3 mm/s and 5 mm/s velocity level were observed at sensor 338.

Table 6 gives the total number of exceedances for several velocity level ranges that were measured by the selection of 59 sensors. The trigger level (1 mm/s) was exceeded 33345 times. The largest portion of these events (94.6%) did not result in an exceedance of the 3 mm/s and 5 mm/s velocity levels. The 5 mm/s velocity level was exceeded 640 times, which is 1.9% of the trigger events. Figure 26 shows that some of these events reached velocity levels much higher than 5 mm/s (up to almost 400 mm/s).

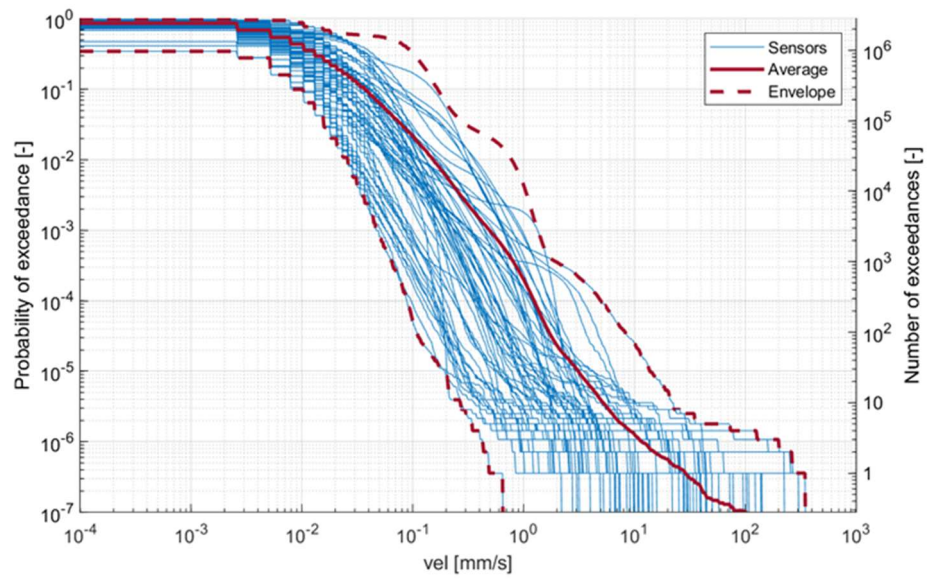


Figure 26 The CCDF curves of the 59 selected sensors based on data from their full operational period.

Table 5 Number of exceedances at five velocity levels for the lower and upper bound of the envelope and the average CCDF for the full operational period of the 59 sensors.

Velocity level	Number of exceedances		
	Minimum	Average	Maximum
0.01 mm/s	278755	1220025.12	2461976
0.1 mm/s	143	60424.93	923473
1 mm/s	0	565.17	12319
3 mm/s	0	30.30	650
5 mm/s	0	10.84	277

Table 6 Total number of exceedances for different velocity ranges observed in the full operational period of the 59 sensors.

Reference velocity [mm/s]	Total exceedances
$0.1 \leq v_{max} < 1mm/s$	3531726
$1 \leq v_{max} < 3mm/s$	31557
$3 \leq v_{max} < 3mm/s$	1148
$v_{max} \geq 5mm/s$	640
$v_{max} \geq 1mm/s$	33345

5.3 Results datasets without likely earthquake-induced heartbeats

The CCDF were also determined for the 59 datasets after removing a subset of heartbeats. These heartbeats measured at the same moment as verified earthquakes by the KNMI and, based on the measured velocity level, are considered likely to be the result of an earthquake.

Figure 27 shows the CCDF of the complete dataset and of the dataset without likely earthquake-induced heartbeats. Similar to the one-year dataset discussed in chapter 4, it is difficult to discern differences between the two graphs. This suggests that for the full operational period of most of the 59 sensors, the contribution of earthquakes to the measured one-minute maximum velocity levels is low.

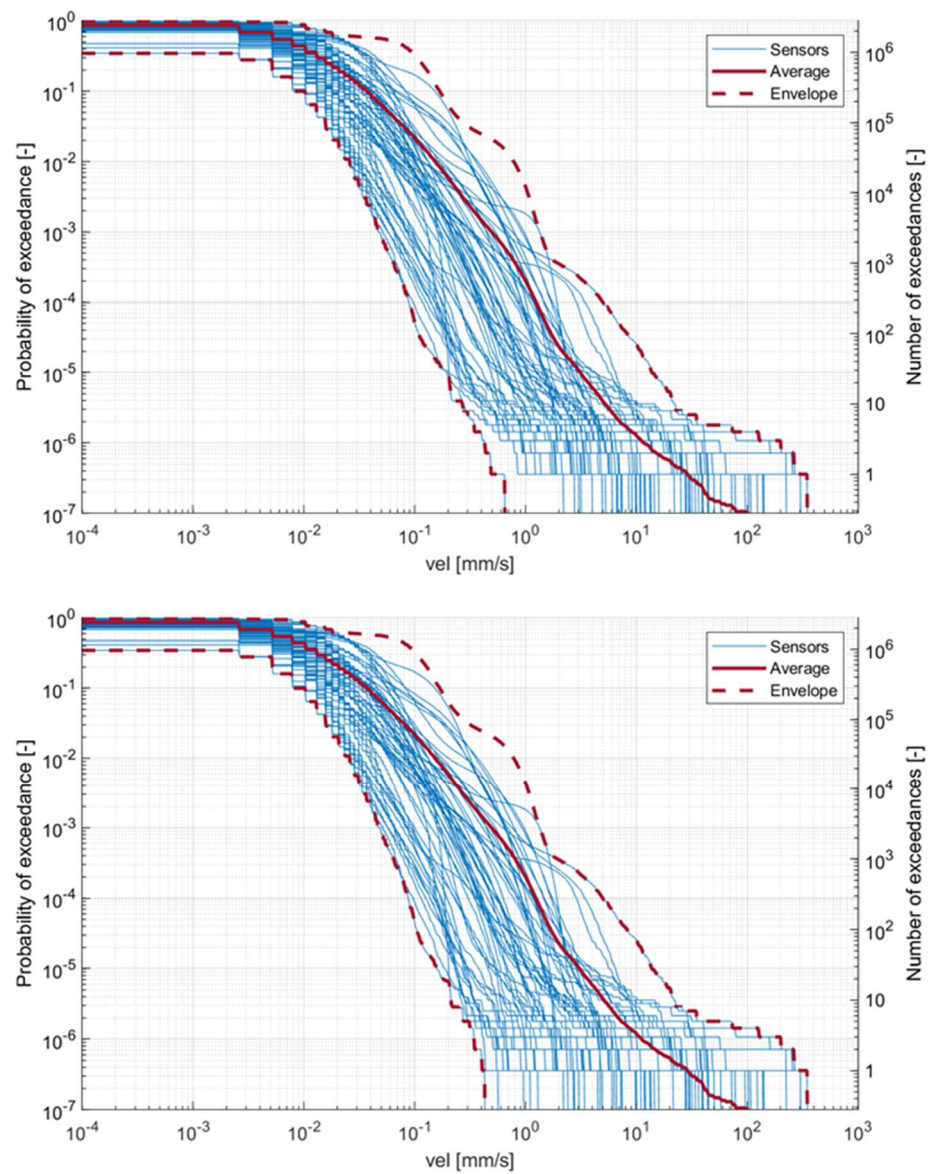


Figure 27 The CCDF curves for the complete datasets (top) and for the datasets without the likely earthquake induced heartbeats (bottom).

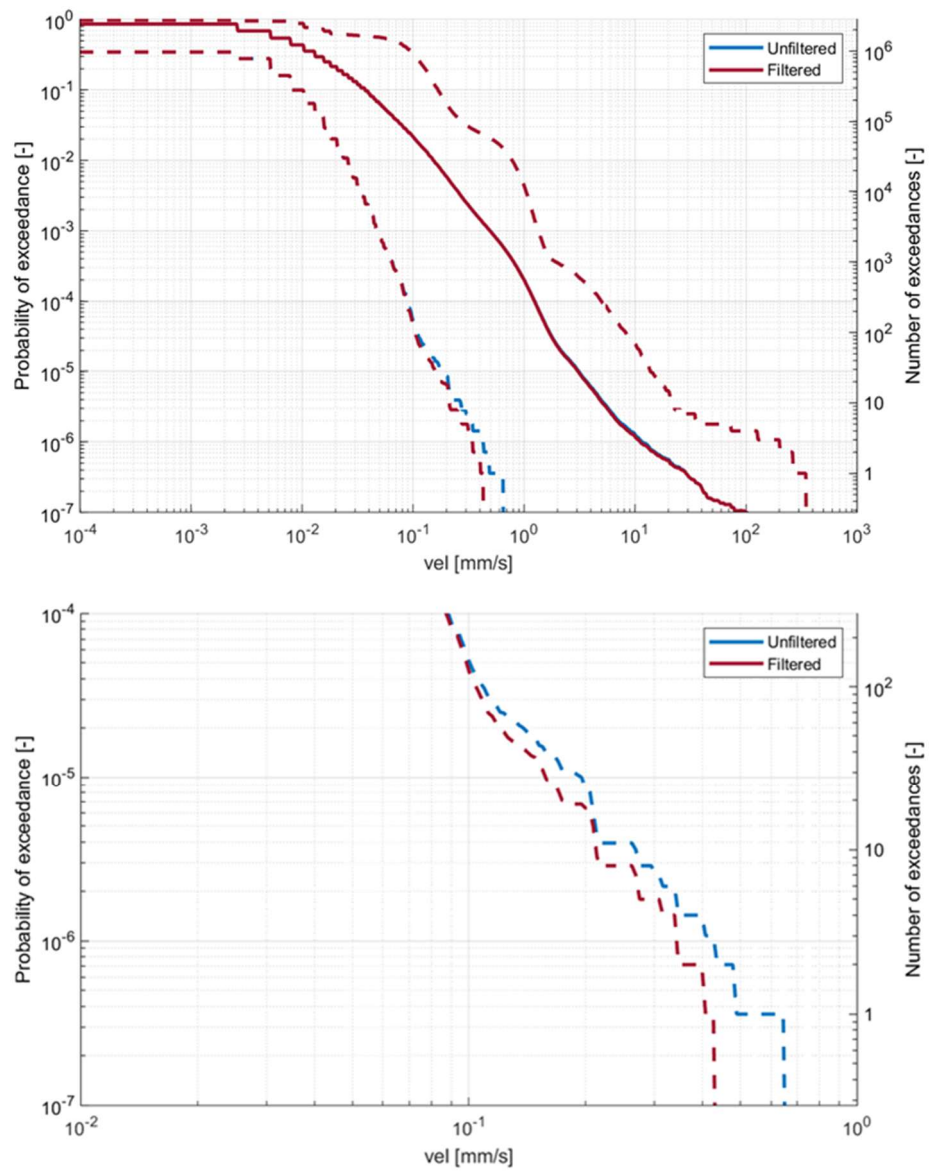


Figure 28 Comparison of average CCDF and lower and upper envelopes for the complete datasets (unfiltered) and for the datasets without (filtered) the likely earthquake induced heartbeats (top). Detail showing the difference between the filtered and unfiltered dataset in the lower envelope (bottom).

Figure 28 (top) presents the average CCDF and the envelope of the two heartbeat datasets. In this graph a difference is observed in the lower envelope, which is shown in more detail in Figure 28 (bottom).

Table 7 gives the number of exceedances of various velocity levels for the average CCDF, and the lower and upper envelope of the two datasets. Small differences are observed for velocity levels of 0.01 mm/s and 0.1 mm/s. For velocity levels of 1 mm/s (the trigger level), 3 mm/s and 5 mm/s no (significant) differences are observed in the number of exceedances for the average CCDF and the lower and upper envelope.

Table 8 gives the total number of exceedances measured by the 59 sensors for various velocity level ranges. Results are provided for the complete dataset (unfiltered) and the dataset without likely earthquake-induced heartbeats (filtered). The last column gives the difference between these two datasets.

For velocity levels above the trigger threshold of the monitoring network (1 mm/s), the difference between the two datasets is 188 heartbeats. This means that 0.6% of the trigger events over the full operational period of the 59 sensors are likely earthquake-induced heartbeats. Table 8 furthermore shows that about 1/3 of these 188 likely earthquake-induced heartbeats (0.16% of all trigger events) exceed 3 mm/s, and that none exceed 30 mm/s.

Table 7 Comparison of the number of exceedances at 5 velocity levels for the lower and upper bound of the envelope and the average CCDF for the full operational period of 59 sensors with (unfiltered) and without (filtered) likely earthquake-induced heartbeats.

Velocity level	Number of exceedances					
	Minimum		Average		Maximum	
	unfiltered	filtered	unfiltered	filtered	unfiltered	filtered
0.01 mm/s	278755	278484	1220025.12	1219411.80	2461976	2460988
0.1 mm/s	143	124	60424.93	60389.54	923473	923274
1 mm/s	0	0	565.17	561.98	12319	12311
3 mm/s	0	0	30.30	29.38	650	650
5 mm/s	0	0	10.84	10.35	277	277

Table 8 Comparison of the total number of exceedances before and after the filtering procedure for different velocity ranges observed in the 1-year dataset

Velocity level	Total number of exceedances (unfiltered)	Total number of exceedances (filtered)	Difference
$0.1 \leq v_{max} < 1mm/s$	3531726	3529826	1900
$1 \leq v_{max} < 3mm/s$	31557	31424	133
$3 \leq v_{max} < 5mm/s$	1148	1122	26
$5 \leq v_{max} < 10mm/s$	429	415	14
$10 \leq v_{max} < 30mm/s$	156	141	15
$v_{max} \geq 30mm/s$	55	55	0
$v_{max} \geq 1mm/s$	33345	33157	188

6 Conclusion

This report describes a study performed on the heartbeat (one minute maximum velocity) data of the monitoring network in Groningen. In order to gain a better understanding of the maximum vibration levels due to sources other than earthquakes, a detailed analysis was performed on the heartbeat data of the sensors in the monitoring network. Two heartbeat datasets were analysed:

- The heartbeat data of 254 sensors in the network for a one-year period with relatively low seismic activity ($M < 2.0$).
- The heartbeat data of 59 sensors for the complete measurement period since instalment of those sensors (about 5 years).

A quality check was performed on both datasets to remove spikes in the data due to calibration and maintenance of the sensor and insufficient datasets. From the heartbeat data, complementary cumulative distribution function (CCDF) curves were extracted to observe the number of exceedances, and probability of exceedance at different velocity values.

To assess the influence of earthquake events, a procedure was developed to determine the heartbeats that correspond with earthquakes verified by the KNMI. The procedure is based on an empirical estimation of the peak ground velocity (PGV) given an earthquake event of a certain magnitude. When a heartbeat velocity, which occurred at the same moment as an earthquake event, is below the upper 95% confidence bound of the estimated PGV, it is assumed to have been the result of the earthquake.

Results for the one-year heartbeat dataset show a total of 9352 exceedances of 1 mm/s, which is the trigger threshold of the monitoring network. On average this corresponds to approximately 37 trigger events per sensor per year. Overall can be concluded that the contribution of likely earthquake-induced heartbeats to the one-year dataset is low. For sensors with relatively low vibration levels (< 1 mm/s) over the one-year period, the removal of likely earthquake-induced heartbeats does have an observable effect on the CCDF curves. However, for velocity levels above the trigger threshold (1 mm/s), only 0.17% of the trigger events measured in the one-year period are likely earthquake-induced heartbeats. None of the likely earthquake-induced heartbeats exceeded 3 mm/s.

Based on the analysis and results of the one-year dataset, a subset of 59 sensors was selected for which the full operation period (approximately 5 years) was analysed. The results of this full operational period dataset show a total of 33345 exceedances of 1 mm/s for 59 sensors which, on average corresponds to ~113 exceedances per sensor per year. Velocity levels of 3 and 5 mm/s were on average exceeded approximately 6 times and 2 times per sensor per year.

Similar to what was observed for the one-year dataset, the contribution of likely earthquake-induced heartbeats to the full operational period dataset of 59 sensors is low. Small differences are observed for velocity levels of 0.01 mm/s and 0.1 mm/s. For velocity levels of 1 mm/s (the trigger level), 3 mm/s and 5 mm/s no significant differences ($< 1\%$) are observed in the number of exceedances between the dataset with and without likely earthquake-induced heartbeats.

7 References

- [1] Borsje, H., Langius, E., Monitoring Network Building Vibrations, TNO 2015 R10501, 2015.
- [2] Borsje, H., Pruiksmā, J.P., Vasic, M., Monitoring Network Building Vibrations – Analysis Earthquake 08-01-2018 (Zeerijp), TNO 2018 R10743-B, 2018.
- [3] <https://www.groningenbereikbaar.nl/nieuws/geen-treinen-van-16-tot-29-oktober-tussen-groningen-buitenpost-en-groningen-delfzijleemshaven>, xxx.
- [4] Bommer, J.J., Stafford, P.J., Ntinalexis, M., Updated empirical GMPEs for PGV from Groningen earthquakes, NAM, 2019.
- [5] SBRCURnet, SBR Trillingsrichtlijn A: Schade aan bouwwerken, Delft, 2017.

8 Signature

Delft, 12-02-2020

Project Leader
Structural Dynamics

Head of Department
Structural Dynamics

A Processing datasets full operational period

This appendix describes the processing performed on the datasets of the selection of 59 sensors.

A.1 Selection of sensors with 5+ year operational period

Since the sensors that are part of the monitoring network were not installed at the same time, the measurement periods vary between sensors. In order to compare heartbeat data from different sensors, the probability of exceedance has been computed with respect to the oldest sensor installed.

The reference number applied in the calculation of the probability of exceedance was set as the number of datapoints that should be recorded by the oldest sensor based on its moment of installation. This is obtained by counting the number of minutes between the first and last measure available of the oldest sensor.

For the selected sensors, the oldest among them is nr. 338, which covered 2789752 minutes (5.308 years). This number also represents the maximum theoretical number of exceedances achievable. Sensor 343 was excluded since its heartbeat contained only around 3 days of data.

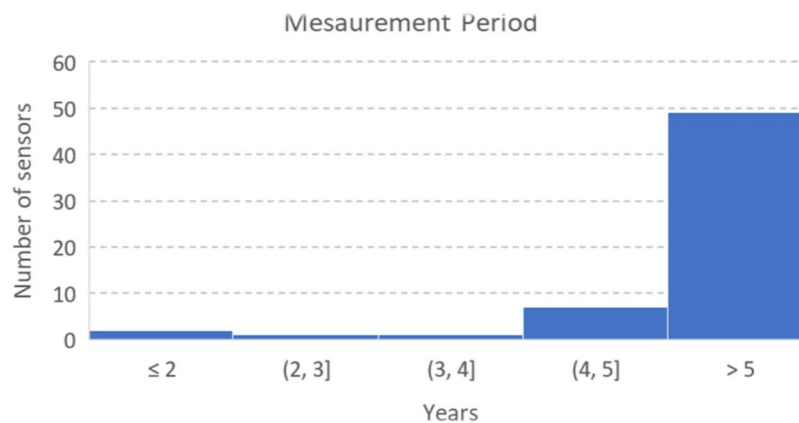


Figure A.1 Distribution of period lengths for the selected sensors.

A.2 Heartbeat spikes due to calibration and maintenance

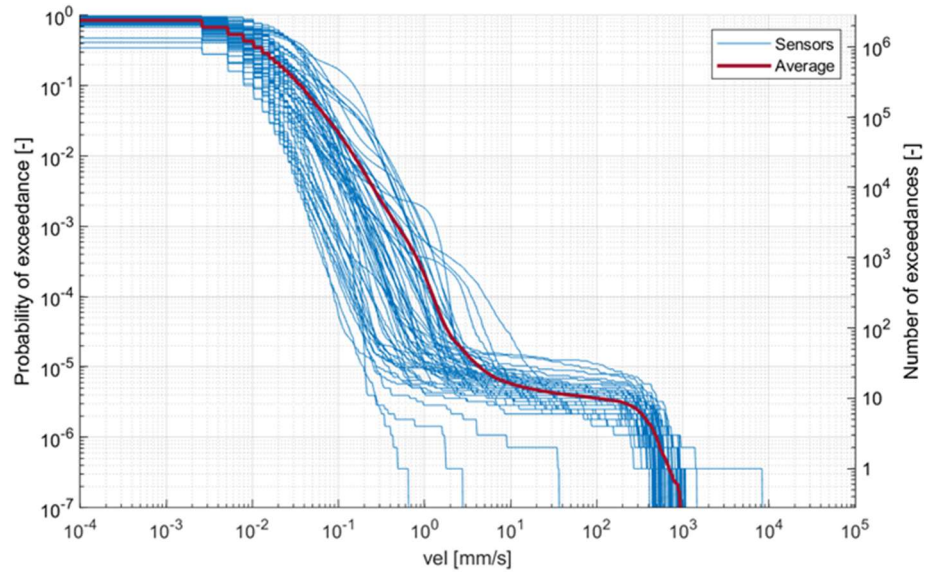


Figure A.2 Envelope of the heartbeat data: the average CCDF (red) and the CCDF of the sensors (solid blue). In the bottom left corner a clear example of a CCDF with insufficient data, on the right a group of CCDF curves with very large vibration levels.

The envelope obtained from the raw heartbeat data is shown in Figure A.2. As was already for the 1-year dataset, spikes are present in the dataset which need to be filtered. The filter of the spikes has been tuned based on the distribution of the maximum velocity for all the sensors. In Figure A.3 a gap is seen in the data between maximum velocities below 300 and above 400 mm/s. The threshold for such analysis has been put at 400mm/s. The resulting envelope after filtering the spikes is shown in Figure A.4.

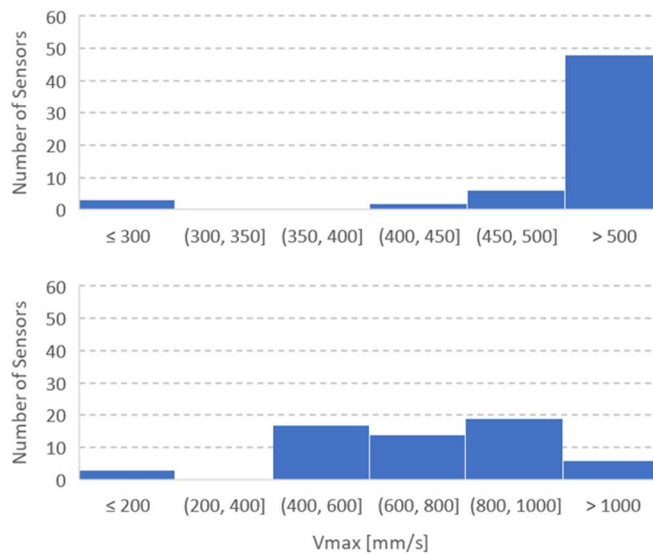


Figure A.3 Distribution of the maximum velocity of all the heartbeat data of the full operational period of the 59 selected sensors. In the top figure, the gap between the spikes and normal trigger level is shown while in the bottom the distribution of the maximum velocity of the spikes is presented.

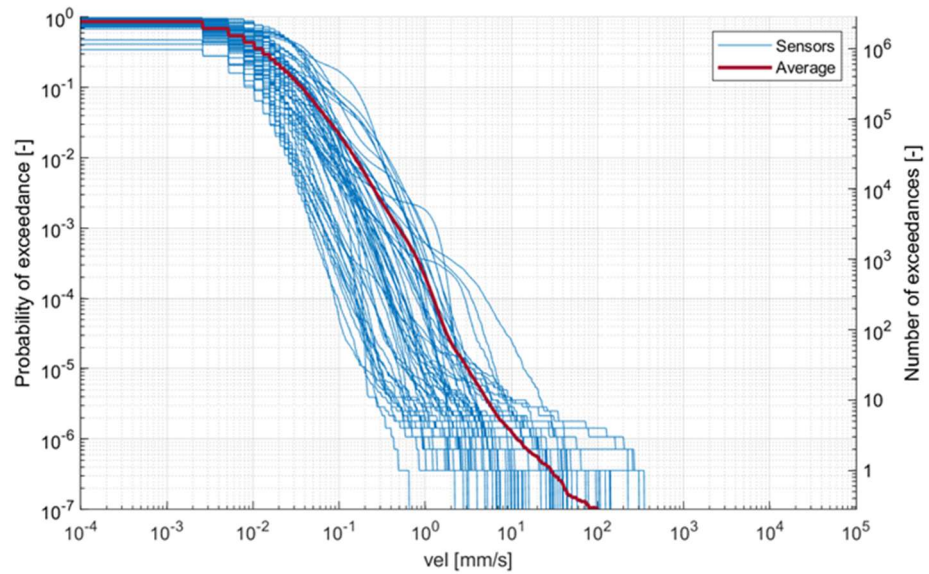


Figure A.4 Envelope of the heartbeat data after removal of the spikes: the average CCDF (red), the CCDF of sensor 15 (dotted blue) and of the other sensors (solid blue).

A.3 Period coverage of selected sensors

The quality of the file is checked considering the ratio between the theoretical and effective number of minutes recorded by the sensors, which is the amount of datapoints contained in the heartbeat. The distribution of the percentages for the dataset is shown in Figure A.5. A percentage higher than 90% was considered sufficient and hence no other sensor were removed from the original dataset of 60 sensor.

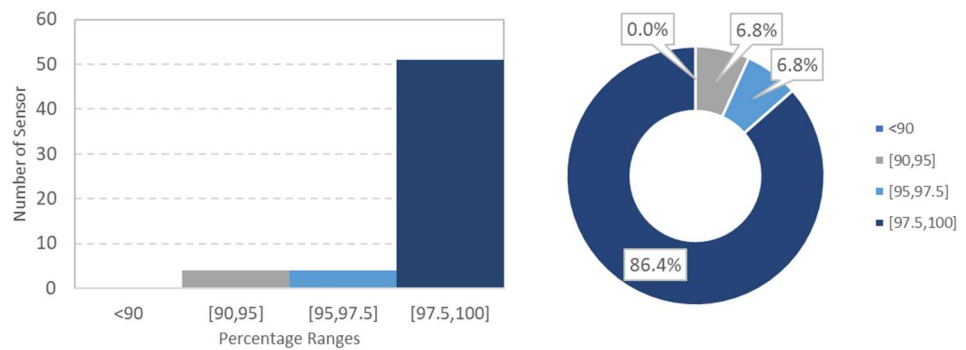


Figure A.5 Distribution of the completeness percentage for the 59 sensors available.